TITLE

# A THEORY FOR DILUTE MAGNETIC ALLOYS — THE ORIGIN OF MAGNETIC ANISOTROPY

AUTHOR

MD ABDUS SATTER

INSTITUTION and DATE

University of Warwick
1989

# A THEORY FOR DILUTE MAGNETIC ALLOYS — THE ORIGIN OF MAGNETIC ANISOTROPY

by

MD ABDUS SATTER B.Sc (Hons.) M.Sc

A Thesis submitted to the

University of Warwick

for the degree of

Doctor of Philosophy

Department of Physics

University of Warwick

Coventry CV4 7AL

October 1989

# ABSTRACT

In this thesis, a formalism for studying the anisotropic interaction between two substitutional magnetic impurities and the magnetic anisotropic effect in a dilute noble metal-transition metal magnetic alloy has been developed from relativistic scattering theory. The theoretical development and the computational techniques of this formalism are based on relativistic spin-polarised scattering theory and relativistic band structure frameworks. For studying the magnetic anisotropic effect a convenient 'working' frame of reference with its axes oriented along the fcc crystal axes is set up. This formalism is applied to study the situation for two Fe impurities in both paramagnetic Au (heavy) and Cu hosts. For AuFe dilute alloy, the two impurity site interaction as a function of separation is not oscillatory and the anisotropic effect is found to be less than the two site interaction itself only by an order of magnitude. Apart from the anisotropic coupling of the two impurity spins to the separation vector, for the first time, another weak anisotropic coupling to the crystal axes is also contained in the two site interaction. These anisotropic effects are the results of the relativistic spin-orbit interaction which are incorporated into the formalism.

# ACKNOWLEDGEMENTS

I would like to thank my supervisor, Dr. J B Staunton, for her excellent supervision, encouragement and help during this study. I would also like to thank my friends Andew Reynolds, Mark Smith and Adrian Wander for their help to introduce me to the University computer and for sharing many enjoyable moments. I am grateful to the Department of Physics for providing me with computer facilities. For financial support, I am also grateful to the Commonwealth Scholarship Commission in the U.K. Finally, I would like to thank my wife for her encouragement.

# DECLARATION

This thesis is submitted to the University of Warwick in support of my application for admission to the degree of Doctor of Philosophy. This thesis contains an account of my own independent research work carried out in the Department of Physics at the University of Warwick from October 1986 to September 1989 under the supervision of Dr. J B Staunton. No part of this thesis has been previously submitted for a degree to anywhere.

# Contents

# List of Tables

# List of Figures

# Chapter 1

## 1.1 Introduction to the thesis

Qualitative microscopic theories for studying magnetism started with the invention of the quantum mechanical Heisenberg model. According to this model, the interaction energy between atomic spins $\underline{S}_i$ and $\underline{S}_j$, $E_{ex.} = -2J_{ij}\underline{S}_i.\underline{S}_j$, is the result of the exchange effect between the two atomic charges on sites $i$ and $j$ and this is sometimes called the direct exchange interaction (Kittel 1976). The origin of this quantum mechanical exchange effect is the Coulomb interaction between the two atomic spins. The exchange parameter $J_{ij}$ is the function of the separation between $\underline{S}_i$ and $\underline{S}_j$ i.e. $J_{ex.} = J_{ij}(r_{ij})$ and it is strongly related to the overlapping of the two atomic charges on sites $i$ and $j$. The nearest neighbour values of $J_{ex.}$ determines whether the ground state of a system is ferromagnetic ($J_{ex.} > 0$) or antiferromagnetic ($J_{ex.} < 0$). This Heisenberg model is useful in almost all of the problems of magnetism in insulators and semiconductors. But this model is not appropriate for the study of magnetism in metals, especially Fe, Co, Ni and their alloys. To study magnetism in transition metals the band approach, usually referred to as the itinerant electron picture, has an important role. In this itinerant model each d electron is assumed to be a Bloch wave or in a band state and according to the simplified Stoner model (1938) the electron-electron exchange is treated in a meanfield (i.e each electron feels the same, average field in the system) approximation. The band of a 'spin-up' electron is treated separately from the band with 'spin-down' electrons. Thus a density of states for 'spin-up' $(+1/2)$ is different from the density of states for 'spin-down' $(-1/2)$. In fig.1.1

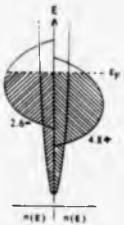


Figure 1.1: Density of states versus energy for Fe. (Bralsford 1966)

the density of states for Fe is shown schematically as a function of energy using the Stoner model (A more realistic calculation is given in Moruzzi, Janak, Williams 1978). The lower energy 3d subband is populated with 4.8 electrons and the higher energy subband is populated with 2.6 electrons. A net spin of 2.2 electrons per atom contributes to the resultant magnetic moment in Fe. The band structure of a transition metal consists of a fairly narrow d-band (compared to the s-band) with a correspondingly more peaked density of states and a broad overlapping sp-band. In discussing magnetic properties, the d-band is important and ferromagnetism (e.g for Fe, Ni, Co) is believed to be produced predominantly by the exchange interactions between the itinerant d-electrons (Herring 1966).

There is another indirect exchange interaction which is the origin of magnetism in rare earth metals (partially filled f-shells shielded by s-p orbitals) especially at low temperatures. The usual picture of this indirect exchange is that the spins of the localized f-electrons associated with one atom polarize the spins of the surrounding conduction electrons by direct exchange and these spin-polarised electrons in turn interact with other localized f-electrons on another atom. Thus the information from one localized f-electron on one atom is transferred to another.This indirect exchange interaction can be modeled by the RKKY (Ruderman and Kittel 1954, Kasuya 1956,Yoshida 1957) interaction. For

many years, the RKKY interaction between two magnetic impurities has been used also to study metallic alloys with a low concentration of magnetic impurities (e.g small amount of iron in gold). This RKKY interaction is of long range oscillatory type and this long range and sign oscillation has an important role in describing spin-glass behaviour of dilute alloys. Details about this RKKY interaction and spin glasses are presented in section 1.2. Owing of the inability of the RKKY interaction to describe any anisotropic coupling between the local magnetic impurity spins the RKKY interaction cannot take into account magnetic anisotropic effects in dilute alloys.

Magnetic anisotropy is a phenomenon for which the spontaneous magnetization of a magnetic material, in the absence of an external field, has a specific direction with respect to the crystal axes and the interaction energy, which is responsible for this preferred direction of magnetization, is called the anisotropic interaction energy. In general magnetic anisotropic interactions are very important in determining domain wall structure, the equilibrium direction of magnetization, magneto-elastic forces and coercive forces. Classically the dipole-dipole interaction is the origin of a magnetic anisotropy. It has now been recognised (Dzyaloshinsky 1958, Moriya 1960, Kondorskii et al 1973) that the anisotropic effect also has a relativistic origin. The spin-orbit interaction term derived from the relativistic Dirac equation (Schiff 1968) is responsible for a magnetic anisotropic effect. Details about such magnetic anisotropy are presented in section 1.3. Stevens (1953) first derived an anisotropic exchange interaction which contains the term $\underline{D}.(\underline{S}_1 \times \underline{S}_2)$ by considering the spin-orbit interaction in the Heisenberg exchange interaction ($\underline{D}$ is related to the separation vector between the spins $\underline{S}_1$ and $\underline{S}_2$). Dzyaloshinsky (1958) pointed out the anisotropy related to the magnetic system from purely symmetry grounds and suggested that an interaction of the form $\underline{D}.(\underline{S}_1 \times \underline{S}_2)$ is responsible for the weak ferromagnetism in $\alpha - Fe_2O_3$ (Hermatite). Moriya (1960) then developed a mechanism for an interaction of the form $\underline{D}.(\underline{S}_1 \times \underline{S}_2)$ (the D.M term) using the Anderson Hamiltonian in his work throughout the calculation and treating the spin-orbit interaction as perturbation. Kondorskii and Straube (1973) studied the anisotropy of nickel also by introducing

spin-orbit interaction as a perturbation in the system. Recently, Fritsche et al (1987) and Strange et al (1989) calculated the magnetocrystalline anisotropy energy for iron and nickel respectively. Strange et al (1989) used the relativistic spin-polarised scattering theory (Strange et al 1984) in their calculation. The spin-orbit coupling links the spin of an electron to the crystal field and thus the magnetic anisotropic effect can arise from the relativistic spin-orbit interaction.

The two site relativistically based anisotropic RKKY interaction may also be very important in studying various properties of dilute magnetic alloys. Fert and Levy (1980), Goldberg and Levy (1986) in their papers have shown how the anisotropy field of a spin-glass can arise from an additional term, as well as the RKKY interaction, which is of the D.M type i.e

$$E_{D.M} \propto R_{12}.(\hat{S}_1 \times \hat{S}_2) \tag{1.1}$$

In their approach, they considered the interaction between two magnetic impurities via spin-orbit scattering from a third site. They used perturbation theory in their approach and effectively they derived a three site interaction. They studied the anisotropic effect in both AuFe and CuMn spin-glass alloys. Later on, Staunton et al (1988) derived an interaction between two magnetic sites mediated by a relativistic electron scattering between them in a uniform positively charged background. In their paper, they studied this relativistic RKKY interaction between two magnetic impurities within a relativistic spin-polarised scattering framework (Strange et al 1984) and presented calculations of the anisotropic component ($E_{12}^{\uparrow\uparrow} - E_{12}^{\uparrow\downarrow}$) for two Fe impurities. This relativistic RKKY interaction contains anisotropic components through a polynomial dependence upon a squared D.M type term and a pseudo-dipolar term ($(\hat{R}_{12}.\hat{S}_1)(\hat{R}_{12}.\hat{S}_2)$) apart from being a function of an isotropic ($\hat{S}_1.\hat{S}_2$) term. They have concluded their paper suggesting an enhanced anisotropy, due to the incorporation of the host realistically, compared to their result $\sim 10^{-06}$ Rydberg. In this thesis, the relativistic effects of the paramagnetic host are incorporated into the interaction between two magnetic impurities. This introduces qualitatively new features to the form of the magnetic anisotropy of such dilute alloys.

In this work, as a first step, the relativistically generalized integrated density of states for a host system with two substitutional magnetic impurities is subtracted from that of the host system alone within a multiple scattering theory framework (Lloyd and Smith 1972). This induced integrated density of states for the two substitutional impurities is used to derive the expression for the relativistic interaction between two magnetic impurities in a realistic host. A relativistic spin-polarized scattering theory (Strange et al 1984) framework forms the basis. Finally, the relativistic interaction between two Fe impurities in a cubic fcc Au-host, its anisotropic components, the anisotropic effect with respect to both crystal axes and the separation vector $\underline{R}_{12}$ and the effective exchange parameter are calculated. Gold is a heavy paramagnetic system, for which the spin-orbit interaction is strong, so AuFe is an interesting dilute alloy to study the consequent anisotropy. The anisotropic effect is also studied for two iron impurities in a paramagnetic copper host, for which the spin-orbit interaction is less strong than gold and a comparison is made with that of the AuFe system. In this work, the relativistic scattering effects due to both host sites and the impurity sites are considered. As a result, the anisotropic features of the interaction between two magnetic impurities in such a host is substantially enhanced.

## 1.2 The RKKY Interaction and Spin-glasses

Frohlich and Nabarro (1940) suggested that the contact hyperfine interaction between conduction electrons and nuclear moments could lead to a polarisation of nuclear moments. After this, the exchange interaction between conduction electrons and localised electronic moments was thought to be the origin of ferromagnetism in transition metals (Zener 1951). Ruderman and Kittel (1954) first calculated the actual form of the indirect exchange type interaction between nuclear magnetic moments $I_i$ and $I_j$ in metals by means of the contact hyperfine interaction of $I_i$ and $I_j$ with the conduction electrons and showed that this interaction leads to broadening of nuclear magnetic resonance absorption. Later on, to study the ferromagnetic properties of transition metals - the exchange interaction between conduction electrons and the localised magnetic moments (arising from unfilled inner d-

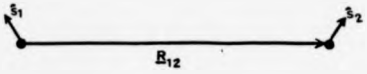


Figure 1.2: Two impurity spins $\vec{S}_1$ and $\vec{S}_2$ (unit vectors) separated by a distance vector $\vec{R}_{12}$.

shell electrons) setting up an indirect coupling between localized magnetic moments was investigated by Kasuya (1956). In the following year, Yoshida (1957) used this interaction to explain the magnetic properties of CuMn alloys. This indirect interaction between two magnetic moments in a metallic host set up by conduction electrons is called the RKKY (Ruderman and Kittel 1954, Kasuya 1956, Yoshida 1957) interaction. Alexander and Anderson (1964) derived the RKKY interaction for metals from a Friedel-Anderson model of the localized moments (Friedel 1958, Anderson 1959). They used a Green's function formalism and treated the s-d exchange interaction in a Hartree-Fock approximation. In scattering theory terms, the RKKY interaction can be seen as an interaction between two impurity potential scatterers set up by the conduction electrons which are described by a plane wave, scattering between the two impurity scattering potentials. The general form of the RKKY interaction is

$$E_{12} \propto \frac{\vec{S}_1 \cdot \vec{S}_2}{R_{12}^3}(2k_f R_{12}\cos(2k_f R_{12}) - \sin(2k_f R_{12})) \tag{1.2}$$

where $\vec{S}_{1(2)}$ is the unit vector along the direction of the magnetic moment for one of the impurity sites, $\vec{R}_{12}$ is the distance vector between $\vec{S}_1$ and $\vec{S}_2$ (as in fig 1.2) and $k_f$ is the Fermi wave vector appropriate to the host. This RKKY interaction decays as the impurities are further separated. It gives a spatially oscillating interaction between the two localized magnetic impurities implanted in a metallic host. The RKKY interaction has

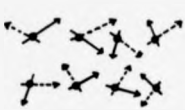

Figure 1.3(a): Paramagnetism: The spins are not frozen; they fluctuate in time (dotted lines).

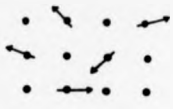

Figure 1.3(b): Spin glass: The spins are frozen into random orientations (comparing fig.1.3(a)).

played an important role in the development of the theory of magnetism and spin-glasses (Edwards and Anderson 1975, Walstedt and Walker 1981).

Examples of spin-glasses are noble metallic alloys, such as AuFe or CuMn, containing between 0.1 and 20 percent of magnetic atoms in the simplest cases and which do not exhibit any long range magnetic order even at low temperatures. The first spin-glass property was observed while studying a dilute alloy of iron in crystalline gold metal (Cannela and Mydosh 1972) and fairly sharp peak was observed at a spin-glass temperature $T_g$ in the susceptibility $\chi$ versus temperature T measurements. Below the spin-glass temperature $T_g$ the spins of the Fe impurity atoms which replace, in a random manner, some of the Au atoms at the normal fcc crystal sites are frozen by their mutual interactions into fixed but random directions i.e in a glassy fashion (fig.1.3(b)). The behaviour of spin-glass alloys has been analysed with the assumption that the magnetic impurities in a metallic host interact in a RKKY form (Edwards and Anderson 1975, Walstedt and Walker 1981). As already mentioned, the RKKY interaction is unable however to describe any anisotropic coupling between the local magnetic moments and thus is inadequate to describe some of the properties of the dilute magnetic alloys and their spin-glass properties. Walstedt and Walker (1981) indicates that a cusp in the susceptibility versus temperature curve for a dilute spin-glass can be obtained if the dipolar anisotropy is included in RKKY interac-

tion. However, the magnetic dipolar interaction is too small to produce the observed cusp (Walstedt and Walker 1981). Monod et al (1979) and Prejean et al (1980) did a series of measurements on the magnetic hysteresis properties of CuMn alloys and CuMn alloys containing a small percentage of Au or Pt in the spin glass states. In their measurements, shifted hysteresis loops, which were square in shape together with jumps in the remanent magnetization (the locked magnetization at zero applied field) were observed and they suggested an existence of anisotropy which maintains the remanent magnetization. As already mentioned, Fert et al (1980) and Levy et al (1981) derived a D.M. type interaction between two magnetic impurity pairs via spin-orbit scattering on a third non-magnetic impurity site and stated that this D.M. type anisotropic effect could explain the existence of remanent magnetization in spin glasses. Goldberg et al (1987) (which has also been mentioned earlier) deduced the D.M. type interaction for binary spin glass considering the spin-orbit scattering on a third identical impurity site. None of these authors could satisfactorily explain the origin of anisotropy which could lead to the existence of remanent magnetization. The anisotropic effects, in their papers, are effectively contained in a three sites interaction and the effects of all the host sites are not incorporated in their calculation. In this thesis, the origin of anisotropic effect is studied deriving an expression for the relativistic interaction between two substitutional magnetic impurities treating the paramagnetic host sites realistically.

## 1.3 Magnetic Anisotropy

As mentioned earlier, magnetic anisotropy can also be defined as the dependence of the internal energy on the direction of the spontaneous magnetization. It describes the circumstance that the energy of a system changes with a rotation of magnetization as in fig.1.4 (Chikazumi 1964). Experimentally, it is found for ferromagnetic materials, such as Fe, Ni, Co, that there are some crystallographic axes along which the magnetization (i.e the magnetic moments tend to align) is possible with lower energy than the other axes (Kittel 1976) and these axes are called easy directions. For Fe the easy axis is a [100]

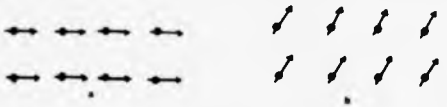

Figure 1.4 Rotation of magnetization (Chikazumi 1964).

direction (Kittel 1976). The difference in energy associated with the easy direction and a certain direction with respect to the easy direction is called the anisotropy energy. Magnetic anisotropy can be measured using a vibrating sample magnetometer. Anisotropy for magnetic alloys can be measured using electron spin resonance measurements.

For the simple case of two magnetic impurities in a non-magnetic host a theoretical model for magnetic anisotropy is developed on the assumption that the interaction between the two magnetic moments $\underline{S}_1$ and $\underline{S}_2$ is dependent on the direction of the relative distance vector $R_{12}$ as well as being dependent on the relative orientation of $\underline{S}_1$ and $\underline{S}_2$ (e.g $S_1.S_2$). The classical magnetic dipole-dipole interaction between the two ionic magnetic moments separated by $R_{12}$ (White 1970)

$$I_{dd} \propto \frac{1}{R^3}[\underline{S}_1.\underline{S}_2 - 3(\underline{S}_1.\hat{R}_{12})(\underline{S}_2.\hat{R}_{12})] \tag{1.3}$$

contributes to the directional dependence of the interaction energy. This magnetic dipole-dipole interaction energy cannot account for the observed magnitude of the anisotropy in many cases. The other important source of the magnetic anisotropy is the coupling between the spin and the orbital motion of the same electron. The orbital motion of an electron in an electric field (due to the ionic crystal sites) produces a magnetic field. The interaction between the spin of the electron with the magnetic field due to its own orbital motion i.e the relativistic spin-orbit interaction links the spin of the electron to the crystal field and thus contributes to the anisotropic effect. Due to the incorporation of the spin-orbit interaction, the relativistic RKKY interaction contains an anisotropic effect

in it and can be interpreted in pseudo-dipolar terms or Dzyaloshinsky-Moriya terms or both (Dzyaloshinsky 1958, Moriya 1960, Levy et al 1981, Goldberg et al 1986, Staunton et al 1988). For example the anisotropic components $(E_{12}^{\uparrow\uparrow} - E_{12}^{\uparrow\uparrow -})$ between the two magnetic moments can be obtained by subtracting the interaction energy with the two moments parallel to $\hat{R}_{12}$ from that with the moments perpendicular to $\hat{R}_{12}$. The two site relativistically based anisotropic RKKY interaction may also be important in studying various properties of spin-glass.

## 1.4 Outlines of the thesis

In chapter 2, following a brief introduction to scattering theory the relativistic spin-polarized scattering theory (Strange et al 1984) is studied. This theory is the framework, within which the relativistic two site interaction and the anisotropic interaction are studied in a later chapter.

In chapter 3, a review of relativistic band structure calculations is presented to examine relativistic effects on systems with high atomic number. As an illustration of the relativistic effects on a pure metallic system of high atomic number, a relativistic and non-relativistic band structure calculation on gold are shown.

In chapter 4, the non-relativistic RKKY interaction is derived using multiple scattering theory (Lloyd and Smith 1972). The relativistic RKKY interaction between two magnetic impurities and the anisotropic interactions studied by Staunton et al (1988) in a uniform positive charged background are also summarized in this chapter.

In chapter 5, the relativistic interaction between two magnetic impurities in a realistic crystalline host is derived and is the main result of this thesis.

In chapter 6, once the computational procedures to study the relativistic interaction derived in chapter 5 and the anisotropic interaction have been described, explicit calculations of interactions including their anisotropic components between Fe impurities in both Au and Cu hosts are shown separately. A substantially enhanced anisotropic effect is found in this calculation over that of two Fe impurities in a uniform background

(relativistic jellium model).

In chapter 7, a conclusion of the thesis is presented and some ideas for future work are also added.

# Chapter 2

# THEORY OF SCATTERING

## 2.1 Introduction

Scattering theory has played an important role in developing theories for both metal and metallic alloys. The most important parameter deduced from scattering theory, the phase shift (see section 2.2), is an essential ingredient for studying the electronic structure of metals and metallic alloys. The muffin-tin potential is expected to be an adequate description of the lattice potential in a metallic system having a close-packed (bcc, fcc, hcp) structure and negligible lattice distortion. The famous KKR (Korringa 1947, Kohn, Rostoker 1954) energy band theory was formulated within the scattering theory framework based on the idea of the closed-packed system, considering the scatterers on all the atomic sites, as spherically symmetric muffin-tin potentials. Relativistic effects in scattering theory i.e strong spin-orbit interaction are expected to be important for heavy atoms, such as gold, since the strong atomic potential can induce extremely large local electron velocities. In developing the KKR energy band theory, a periodic array of muffin-tin potential scatterers and the powerful Green's function formalism are considered in a multiple scattering theory approach.

In section 2.2, the non-relativistic scattering theory for a single site potential is discussed. In section 2.3, the relativistic spin-polarised scattering theory is presented for a muffin-tin potential with the magnetic component of the potential oriented along the Z-


Figure 2.1: The muffin-tin potential $v(r)$ and $V_{MTZ}$ is the muffin-tin zero. $r_{MT}$ is the muffin-tin radius at which the potential is truncated to $V_{MTZ}$.

axis of the local coordinate frame attached to a single site (Strange et al 1984). Staunton et al (1988) studied the relativistic RKKY interaction and the anisotropic effect between two magnetic impurities implanted in a jellium model using this relativistic spin-polarized scattering theory. The main aim of this thesis is the derivation and study of the anisotropic component for the interaction between two magnetic impurities in a realistic paramagnetic host and is also formulated within this relativistic spin-polarized scattering theory framework following the work of Strange et al (1984). In section 2.4, multiple scattering theory is summarized.

## 2.2 Scattering theory for a single scatterer

For a single spherically symmetric muffin-tin potential, the solution to the time independent Schrodinger equation (Gyorffy and Stocks 1979) in atomic units (a.u)

$$[-\nabla^2 + v(r)]\Psi(\underline{r}) = E\Psi(\underline{r}) \tag{2.1}$$

can be written in the form

$$\Psi(\underline{r}, E) = \sum_L a_L(E) R_l(r, E) Y_L(\theta, \phi) \tag{2.2}$$

where $Y_L(\theta, \phi)$ is a spherical harmonic with orbital and magnetic quantum numbers $(l, m) \equiv L$ and $R_l(r, E)$ is the solution of the radial equation

$$[-\frac{d^2}{dr^2} - \frac{2}{r}\frac{d}{dr} + \frac{l(l+1)}{r^2} + v(r)]R_l(r, E) = E R_l(r, E) \tag{2.3}$$

This radial Schrodinger equation has the free electron solution for $r > r_{MT}$ and the linear combination of two linearly independent solutions for free electron, such as the spherical Bessel and Neumann functions $j_l(\sqrt{E}r)$ and $n_l(\sqrt{E}r)$ respectively is the radial solution . Therefore, the the radial solution of eq.(2.3) may be written as (Gyorffy and Stocks 1979)

$$R_l(r;E) = \cos\delta_l j_l(\sqrt{E}r) - \sin\delta_l n_l(\sqrt{E}r) \qquad for \qquad r > r_{MT} \tag{2.4}$$

Asymptotically, as $r \longrightarrow \infty$

$$j_l(\sqrt{E}r) \overset{r\to\infty}{\longrightarrow} \frac{1}{\sqrt{E}r}\sin(\sqrt{E}r - \frac{l\pi}{2}) \tag{2.5}$$

and

$$n_l(\sqrt{E}r) \overset{r\to\infty}{\longrightarrow} -\frac{1}{\sqrt{E}r}\cos(\sqrt{E}r - \frac{l\pi}{2}) \tag{2.6}$$

and

$$R_l(r;E) \overset{r\to\infty}{\longrightarrow} \frac{1}{\sqrt{E}r}\sin(\sqrt{E}r - \frac{l\pi}{2} + \delta_l(E)) \tag{2.7}$$

For zero potential i.e $v(r) = 0$, the radial solution of eqn.(2.3) is only the Bessel function, because it is finite at $r \longrightarrow 0$. Therefore, in free space

$$R_l(r;E) = j_l(\sqrt{E}r) \overset{r\to\infty}{\longrightarrow} \frac{1}{\sqrt{E}r}\sin(\sqrt{E}r - \frac{l\pi}{2}) \tag{2.8}$$

which differs from (2.7) only by a shift of phase $\delta_l(E)$. Hence $\delta_l(E)$ is usually referred to as the phase shift, which is a function of energy.

Inside the muffin-tin sphere $R_l(r;E)$ is determined by solving equation (2.3) numerically, which is regular at the origin and at $r = r_{MT}$ its derivative (Loucks 1967)

$$L_l = R_l^{-1}\frac{dR_l}{dr}\Big|_{r=r_{MT}} \tag{2.9}$$

must be equal to the logarithmic derivative of $R_l(r;E)$ on the outside given by eq.(2.4).

From this condition

$$\delta_l = \arctan\left[\frac{\sqrt{E}j_l'(\sqrt{E}r_{MT}) - L_l(E)j_l(\sqrt{E}r_{MT})}{\sqrt{E}n_l'(\sqrt{E}r_{MT}) - L_l(E)n_l(\sqrt{E}r_{MT}}\right] \tag{2.10}$$

In scattering theory, one seeks the solution of eq.(2.1) that will have the form of an incident wave plus a scattered spherical wave. Thus the solution, for points far away from

the scattering centre, has the form

$$\Psi_{\underline{k}}(\underline{r}) = e^{i\underline{k}\cdot\underline{r}} + f(k^2,\theta)\frac{e^{ikr}}{kr} \tag{2.11}$$

where $\theta$ is the angle between $\underline{k}$ and $\underline{r}$ and the scattering amplitude is given by (Schiff 1968)

$$f(E,\theta) = \sum_l (2l+1) f_l(E) P_l(\cos\theta) \tag{2.12}$$

where $f_l(E) = \sin\delta_l(E) e^{i\delta_l(E)}$ and $P_l(\cos\theta)$ is the Legendre polynomial and one can easily show that the total scattering cross-section $\sigma$ is given by (Schiff 1968)

$$\sigma = \frac{4\pi}{E}\sum_l (2l+1)\sin^2\delta_l(E) \tag{2.13}$$

Thus a phase shift near $\pi/2$ means very strong scattering and near 0 or $\pi$ means weak scattering. From eqs. (2.11) to (2.13) it is evident that the phase shifts actually determine the scattering properties of the potential function. In chapter 3, it is obvious that the energy bands of a pure metal depend on the muffin-tin potential only through the phase shifts.

In another representation, the radial solution $R_l(r;E)$ in eq.(2.4) is written as

$$R_l(r;E) = j_l(\sqrt{E}r) - i\sqrt{E}t_l(E)h_l^+(\sqrt{E}r) \qquad for \qquad r > r_{MT} \tag{2.14}$$

Where $h_l^+(\sqrt{E}r)$ is Hankel function defined by $h_l^+(\sqrt{E}r) = j_l(\sqrt{E}r) + in_l(\sqrt{E}r)$ and the parameter multiplying the Hankel function is called the transition matrix or the t-matrix. The t-matrix is represented in terms of the scattering phase shifts $\delta_l(E)$ as

$$t_l(E) = -\frac{1}{\sqrt{E}}\sin\delta_l e^{i\delta_l} \tag{2.15}$$

This $t$-matrix can also be used for describing the scattering properties of a potential instead of phase shifts. A relativistic generalisation of this $t$-matrix is used in chapter(5) to derive the desired interaction between two magnetic impurities. In the next section, an elegant theory developed by Strange et al (1984) and Feder et al (1983) to calculate the relativistic $t$-matrix for relativistic spin-polarized scattering by a potential having a magnetic component is reviewed.

## 2.3 Spin-polarized scattering theory for a single scatterer having a magnetic component

Hohenberg and Kohn (1964) first proved a theorem that the ground state energy of a many-body system, regardless of whether the particles obey the Bose or Fermi statistics, is a unique functional of the density, $n(r)$, and is a minimum when calculated for the true ground-state density. In the following year, Kohn and Sham (1965) showed how a one-particle Schrodinger equation can be set up, which includes all the effects of the correlations and exchange among the particles of the system within the unique density functional approach. This one-particle Schrodinger equation is solved self-consistently and the ground state energy of the many-body problem can be achieved via the one-particle picture. All of these are confined to non-relativistic many body theory. The relativistic generalization of the theory has been developed for systems of large atomic number (Ramana and Rajagopal 1979, MacDonald and Vosko 1979).

In this section, spin-polarised scattering theory (Feder et al 1983, Strange et al 1984) for a muffin-tin potential ($v^{ext.}$) is presented within this relativistic generalization of the Kohn-Sham one-particle Schrodinger equation. This relativistic spin-polarized scattering theory has revealed the opportunity to derive a realistic theory for magnetic anisotropy.

Neglecting diamagnetic effects and using the Gordon decomposition of the current (Baym 1969), the appropriate relativistic Kohn-Sham-Dirac equation can be written as (MacDonald and Vosko 1979, Strange et al 1984)

$$E\Psi = (-i\hbar c\underline{\alpha}.\underline{\nabla} + \beta mc^2 + 1V^{eff}.[n,\underline{m}] + \beta\underline{\sigma}.\underline{B}^{eff}[n,\underline{m}])\Psi \tag{2.16}$$

where

$$n(\underline{r}) = tr\int dEf(E-\nu)\Psi^{\dagger}(\underline{r})\Psi(\underline{r}) \tag{2.17}$$

$$\underline{m}(\underline{r}) = tr\int dEf(E-\nu)\Psi^{\dagger}(\underline{r})\beta\underline{\sigma}\Psi(\underline{r}) \tag{2.18}$$

$$V^{eff}.(\underline{r}) = -(v^{ext.} + \frac{\delta E_{xc}^{R}}{\delta n(\underline{r})} + e^2\int\frac{n(r')}{|\underline{r}-\underline{r}'|}d\underline{r}') \tag{2.19}$$

$$\underline{B}^{eff}.(\underline{r}) = \frac{e\hbar}{2mc}(\underline{B}^{ext.}) + \frac{\delta E_{xc}^{R}}{\delta\underline{m}(\underline{r})} \tag{2.20}$$

and the standard Dirac matrices (Rose 1961) which can be expressed in terms of the conventional 2 × 2 Pauli matrices

$$\underline{\alpha} = \begin{pmatrix} 0 & \underline{\sigma} \\ \underline{\sigma} & 0 \end{pmatrix} \qquad and \qquad \beta = \begin{pmatrix} \bar{1} & 0 \\ 0 & -\bar{1} \end{pmatrix} \tag{2.21}$$

$\underline{B}^{ext}$ is a fictional magnetic field coupling to the current only due to the spin of the electron on the atom. In this approach, coupling to the orbital part of the electron is neglected. $\Psi$ is a four spinor and $E_{xc}^R$ is the relativistic exchange correlation energy (neglecting the diamagnetic effect). Therefore $V^{eff}$ and $\underline{B}^{eff}$ represent a single finite ranged muffin-tin potential with the magnetic component only due to spin. In the notation of Rose (Rose 1961), when both $V^{eff}$ and $\underline{B}^{eff}$ are spherically symmetric and if the magnetic component of the potential is oriented along the Z-axis appropriate to the local coordinate frame attached to this single site, then the Kohn-Sham-Dirac equation in atomic units and polar coordinates (Rose 1961) (in a.u. m=1/2, $\hbar = 1$, $c^2 = 2$) can be written

$$E\Psi = [ic\gamma_5\sigma_r(\frac{\delta}{\delta r} + \frac{1}{r} - \frac{\beta\hat{K}}{r}) + \frac{\beta c^2}{2} + V^{eff}(r) + \beta\sigma_z B^{eff}(r)]\Psi \tag{2.22}$$

$$\text{using } \underline{\alpha}.\underline{p} = -i\alpha_r\frac{\delta}{\delta r} + i\frac{\alpha_r}{r}\underline{\sigma}.\underline{L}, \qquad \underline{\sigma} = -\underline{\alpha}\gamma_5, \qquad \hat{K} = \beta(\underline{\sigma}.\underline{L} + 1)$$

and $V^{eff} = B^{eff}(r) = 0 \qquad r > r_{MT}$

where

$$\alpha_r = \begin{pmatrix} 0 & -i \\ i & 0 \end{pmatrix} \qquad \gamma_5 = -\begin{pmatrix} 0 & \bar{1} \\ \bar{1} & 0 \end{pmatrix} \qquad and \qquad \sigma_r = -\alpha_r\gamma_5 \tag{2.23}$$

and $\underline{L}$ is the orbital angular momentum operator with eigenvalues l, $K$ has eigenstates $\chi_\kappa^{m_j}(\hat{\underline{r}})$ with eigenvalues $-\kappa$. The spin angular function $X_\kappa^{m_j}(\hat{\underline{r}}\eta)$ satisfies (Strange et al 1984)

$$\chi_\kappa^{m_j}(\hat{\underline{r}}\eta) = \sum_{m_s=+1/2,-1/2} C_{m_s,m_j-m_s}^{jm_j} Y_l^{m_j-m_s}(\hat{\underline{r}}) X_s^{m_s}(\eta) \tag{2.24}$$

where $C_{m_s,m_j-m_s}^{jm_j}$ is a Clebsch-Gordon coefficient with $m = m_j - m_s$, $Y_l^m(\hat{\underline{r}})$ is a spherical harmonic and the spin function $X_s^{m_s}(\eta)$ is such that $\sigma_z X_s^{m_s}(\eta) = m_s X_s^{m_s}(\eta)$. The operator $\hat{K}$ commutes with $\underline{J}^2 = (\underline{L} + \underline{S})^2$ (with eigenvalues $j(j+1)$) and its projection $j_z$ (with

eigenvalues $m_j$). The allowed values of $\kappa$ in terms of $l$ and $j$ are

$$\kappa = \begin{cases} +(j+1/2) & \text{if } j = l - 1/2 \\ -(j-1/2) & \text{if } j = l + 1/2 \end{cases} \tag{2.25}$$

This gives for $l \leq 2$

| | | | | | | | | | | |
|---|---|---|---|---|---|---|---|---|---|---|
| $l =$ | 0 | | 1 | | | 2 | | | | |
| $m =$ | 0 | 1 | 0 | −1 | 2 | 1 | 0 | −1 | −2 | |
| $m_s =$ | $+\frac{1}{2}$ | $-\frac{1}{2}$ | $+\frac{1}{2}$ | $-\frac{1}{2}$ | $+\frac{1}{2}$ | $-\frac{1}{2}$ | $+\frac{1}{2}$ | $-\frac{1}{2}$ | $+\frac{1}{2}$ | $-\frac{1}{2}$ | $+\frac{1}{2}$ | $-\frac{1}{2}$ | $+\frac{1}{2}$ | $-\frac{1}{2}$ |
| $\kappa =$ | −1 | 1 | −2 | | 2 | | −3 | | | |
| $m_j =$ | $+\frac{1}{2}$ | $-\frac{1}{2}$ | $+\frac{1}{2}$ | $-\frac{1}{2}$ | $+\frac{3}{2}$ | $+\frac{1}{2}$ | $-\frac{1}{2}$ | $-\frac{3}{2}$ | $+\frac{3}{2}$ | $+\frac{1}{2}$ | $-\frac{1}{2}$ | $-\frac{3}{2}$ | $+\frac{3}{2}$ | $-\frac{3}{2}$ |

In integral form, the solution of (2.22) is (Newton 1966)

$$\Psi(\underline{p}, \underline{r}, m_s) = \Psi_o(\underline{p}, \underline{r}, m_s) + \int d\underline{r}' \bar{G}_o^{\dagger}(\underline{r}, \underline{r}', E)(V^{eff}(r')\bar{1} + B^{eff}(r')\beta\sigma_z)\Psi^{\dagger}(\underline{p}, \underline{r}', m_s) \tag{2.26}$$

where $\Psi_o$ is a four-component free particle plane wave spinor, with momentum $\underline{p}$, which can be written

$$\Psi_o = \sqrt{\left(\frac{p(E+\frac{c^2}{2})}{\pi}\right)} \sum_{\kappa,m_j} \begin{pmatrix} j_l(pr)\chi_{\kappa}^{m_j}(\hat{\underline{r}}) i^l X_{\kappa}^{m_s}(\eta)\chi_{\kappa}^{m_j\dagger}(\hat{\underline{p}}) \\ \frac{ip}{(E+\frac{c^2}{2})} S_{\kappa} j_{\bar{l}}(pr)\chi_{-\kappa}^{m_j}(\hat{\underline{r}}) i^{\bar{l}} X_{\kappa}^{m_s}(\eta)\chi_{-\kappa}^{m_j\dagger}(\hat{\underline{p}}) \end{pmatrix} \tag{2.27}$$

The matrix elements of the advanced free-particle Green function (Rose 1961) spin matrix

$$\bar{G}_o^{\dagger} = \begin{pmatrix} G_{o11} & G_{o12} \\ G_{o21} & G_{o22} \end{pmatrix} \tag{2.28}$$

are

$$G_{o11} = ip(E + \frac{c^2}{2}) \sum_{\kappa,m_j} h_l^{\dagger}(pr) j_{\bar{l}}(pr')\chi_{\kappa}^{m_j}(\hat{\underline{r}})\chi_{\kappa}^{m_j\dagger}(\hat{\underline{r}}')$$

$$G_{o12} = -p^2 \sum_{\kappa,m_j} S_{\kappa} h_{\bar{l}}^{\dagger}(pr) j_{\bar{l}}(pr')\chi_{-\kappa}^{m_j}(\hat{\underline{r}})\chi_{\kappa}^{m_j\dagger}(\hat{\underline{r}}')$$

$$G_{o21} = -G_{o12}$$

$$G_{o22} = [\frac{(E-\frac{c^2}{2})}{(E+\frac{c^2}{2})}]G_{o11} \qquad for \qquad r > r' \tag{2.29}$$

If $r < r'$, then $r$ and $r'$ are interchanged in the spherical Hankel function $h^{\dagger}$ and Bessel functions $j$. The quantum number $\bar{l}$ is related to $l$ by $\bar{l} = l - S_{\kappa}$ and $S_{\kappa} = \kappa/|\kappa|$ and the

energy, $E$ is such that $(E+\frac{c^2}{2})(E-\frac{c^2}{2}) = p^2$. The full solution $\Psi^\dagger$ can also be expanded as

$$\Psi^\dagger(\underline{p},\underline{r},m_s) = \sum_{\kappa,\kappa',m_j,m_j'} \begin{pmatrix} g^{m_j'm_j}_{\kappa'\kappa}(r)\chi^{m_j'}_{\kappa'}(\hat{\underline{r}})i^l X^{m_s}_s(\eta)\chi^{m_j^\dagger}_{\kappa}(\hat{\underline{p}}) \\ if^{m_j'm_j}_{\kappa'\kappa}(r)\chi^{m_j'}_{-\kappa'}(\hat{\underline{r}})i^{\bar{l}} X^{m_s}_s(\eta)\chi^{m_j^\dagger}_{-\kappa}(\hat{\underline{p}}) \end{pmatrix} \tag{2.30}$$

where $g(r)$ and $f(r)$ are the radial solutions of the Dirac equation and (2.30) satisfies the following set of radial differential equations (in atomic units) (Strange et al 1984)

$$[-c\frac{\delta}{\delta r} + \frac{(\kappa_2 - c)}{r}]f^{m_{j2}m_{j1}}_{\kappa_2\kappa_1}(r) + [E - V^{eff}(r) - \frac{c^2}{2}]g^{m_{j2}m_{j1}}_{\kappa_2\kappa_1}(r) + B^{eff}(r)\sum_{\kappa'} G(\kappa_2,\kappa',m_{j2})g^{m_{j2}m_{j1}}_{\kappa'\kappa_1}(r) = 0 \tag{2.31}$$

$$[c\frac{\delta}{\delta r} - \frac{(\kappa_2 - c)}{r}]g^{m_{j2}m_{j1}}_{\kappa_2\kappa_1}(r) + [E - V^{eff}(r) + \frac{c^2}{2}]f^{m_{j2}m_{j1}}_{\kappa_2\kappa_1}(r) - B^{eff}(r)\sum_{\kappa'} G(-\kappa_2,-\kappa',m_{j2})g^{m_{j2}m_{j1}}_{\kappa'\kappa_1}(r) = 0 \tag{2.32}$$

where

$$G(\kappa_2,\kappa',m_{j2}) = tr\int \underline{d\hat{r}}\chi^{m_{j2}^\dagger}_{\kappa_2}(\hat{\underline{r}})\sigma_z\chi^{m_{j2}}_{\kappa'}(\hat{\underline{r}}). \tag{2.33}$$

In atomic units, the velocity of light $c \approx 274$. The first pair of indices $\kappa_2, m_{j_2}$ in equations (2.31) and (2.32) indicates the component of the wave function belonging to these specific values. The second pair $\kappa_1, m_{j_1}$ refers to the corresponding values of the incident beam i.e. the boundary conditions (Newton 1966). The coupling in (2.31) and (2.32), determined by the non-zero values of G in equation (2.33), is for each value of $m_j$ between (1) $j = l + 1/2$ ($\kappa = -l - 1$) and $j = l - 1/2$ ($\kappa = l$) and (2) between $l, j$ and $l \pm 2, j \pm 1$. Neglecting the second coupling (2), equations (2.31) and (2.32) are reduced to a four coupled equations involving $f^{m_j}_{\kappa,\kappa-1}, f^{m_j}_{\kappa-1,\kappa}, g^{m_j}_{\kappa,\kappa-1}$ and $g^{m_j}_{\kappa-1,\kappa}$. This makes their solution much more tractable.

Outside the potential, $r > r_{MT}$, radial solutions to (2.31) and (2.32) can be written in

a column vector form, as (Strange et al 1984)

$$\begin{pmatrix} j_{l_1}(pr)\delta_{\kappa_1,\kappa} - iph^{\dagger}_{l_1}(pr)t^{m_j}_{\kappa_1\kappa}(E) \\ \frac{ip}{(E+\frac{2}{\alpha})}S_{\kappa_1}(j_{l_1}(pr)\delta_{\kappa_1\kappa} - iph^{\dagger}_{l_1}t^{m_j}_{\kappa_1\kappa}(E)) \\ j_{l_2}(pr)\delta_{\kappa_2\kappa} - iph^{\dagger}_{l_2}(pr)t^{m_j}_{\kappa_2\kappa}(E) \\ \frac{ip}{(E+\frac{2}{\alpha})}S_{\kappa_2}(j_{l_2}(pr)\delta_{\kappa_2\kappa} - iph^{\dagger}_{l_2}t^{m_j}_{\kappa_2\kappa}(E)) \end{pmatrix} \tag{2.34}$$

Here $\kappa$ again describes the boundary condition i.e. the value of the orbital and total angular momenta of the component of the incident beam. The solution described by (2.34) outside the potential is then matched at the point $r = r_{MT}$ to solutions inside the spherically symmetric muffin-tin potential with radius $r = r_{MT}$. The solution inside the potential well ($r < r_{MT}$) is

$$\begin{pmatrix} g^{m_j}_{\kappa_1\kappa}(r) \\ if^{m_j}_{\kappa_1\kappa}(r) \\ g^{m_j}_{\kappa_2\kappa}(r) \\ if^{m_j}_{\kappa_2\kappa}(r) \end{pmatrix} = \sum_{\nu} a^{m_j}_{\kappa\nu} \begin{pmatrix} \overline{g}^{m_j}_{\kappa_1\nu}(r) \\ i\overline{f}^{m_j}_{\kappa_1\nu}(r) \\ \overline{g}^{m_j}_{\kappa_2\nu}(r) \\ i\overline{f}^{m_j}_{\kappa_2\nu}(r) \end{pmatrix} \quad \kappa = \begin{cases} \kappa_1, & \kappa_2 \\ l, & -l-1 \end{cases} \quad and \quad \nu = 1, \quad 2 \tag{2.35}$$

To solve the coupled differential equations numerically Strange et al (1984) first found the analytic form of the wave function valid for small $r$

$$\begin{pmatrix} \overline{g}^{m_j}_{\kappa_1\nu}(r) \\ i\overline{f}^{m_j}_{\kappa_1\nu}(r) \\ \overline{g}^{m_j}_{\kappa_2\nu}(r) \\ i\overline{f}^{m_j}_{\kappa_2\nu}(r) \end{pmatrix} \xrightarrow{r \longrightarrow 0} \begin{pmatrix} 1 \\ \rho(\kappa_1) \\ 0 \\ 0 \end{pmatrix} r^{b(\kappa_1)} \quad , \nu = 1$$

$$\begin{pmatrix} \overline{g}^{m_j}_{\kappa_1\nu}(r) \\ i\overline{f}^{m_j}_{\kappa_1\nu}(r) \\ \overline{g}^{m_j}_{\kappa_2\nu}(r) \\ i\overline{f}^{m_j}_{\kappa_2\nu}(r) \end{pmatrix} \xrightarrow{r \longrightarrow 0} \begin{pmatrix} 0 \\ 0 \\ 1 \\ \rho(\kappa_2) \end{pmatrix} r^{b(\kappa_2)} \quad , \nu = 2 \tag{2.36}$$

where $b(\kappa) = \sqrt{[\kappa^2 - (2Z/c)^2]}$ and $\rho(\kappa) = \frac{(\kappa + a(\kappa))}{2Z/c}$, $Z$ being the atomic number appropriate to the potential. A linear combination of (2.36) is also the solution of the coupled differential equations (2.31) and (2.32) at $r \to 0$. Using this initialization for wave function, Strange et al (1984) solved the coupled differential equations (2.31) and (2.32) inside

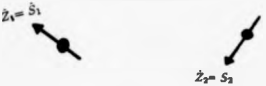


Figure 2.2: Representation of the arbitrary directions of the two spins.

the muffin-tin potential using a generalization of the method given by Loucks (1967). This method involves the Milne integration method (Loucks 1967) to solve the coupled differential equations numerically from $r \to 0$ to $r = r_{MT}$ at the muffin-tin boundary. Now matching this solution to the solution (2.34) outside the muffin-tin boundary the relativistic $t-$matrix is calculated in the representation $t_{\kappa\kappa'}^{m_s m_s'}$. To use this $t$-matrix in the derived expression in chapter (5) for the relativistic interaction between two magnetic impurities, it is convenient to express the relativistic $t$-matrix in $l, m$ and $m_s$ representation by the relation

$$t_{lm m_s, l'm' m_s'} = \sum_{\kappa\kappa'} C_{m,m_s}^{\kappa m_s, m-m_s} t_{\kappa\kappa'}^{m_s m_s'}(E) C_{m',m_s'}^{\kappa' m_s', m'-m_s'} \tag{2.37}$$

where $C_{m,m_s}^{\kappa m_s, m}$ are defined by equation (2.24) and the $t$-matrix satisfies

$$t_{lm m_s, l'm' m_s'} = t_{m,m_s,m+m_s,-m_s';m',m_s',m'-m_s+m_s'}^{l} \delta_{ll'} \delta_{m,m'-m_s+m_s'} \tag{2.38}$$

The same numerical procedure for evaluating the $t$-matrix is used in this work. For the desired relativistic interaction between two magnetic impurities, however, one needs to allow the magnetic component to be oriented along an arbitrary direction (Fig.2.2). The arbitrary coordinate frame is set up by rotating through Euler angles $\alpha, \beta, \gamma$ the "local" coordinate frame (the frame with its $Z$-axis set up along the magnetic component of the potential). The Euler angle rotation is the result of the following sequence of three relations: (Messiah 1965)

(1) a rotation of angle $\alpha$ about $OZ$, $R_Z(\alpha)$ ($OY$ goes into $OU$)

(2) a rotation of angle $\beta$ about $OU$, $R_U(\beta)$ ($OZ$ goes into $OZ'$)

(3) a rotation of angle $\gamma$ about $OZ$, $R_Z(\gamma)$ ($OU$ goes into $OY'$)

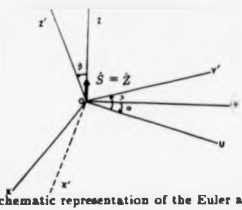


Figure 2.3: Schematic representation of the Euler angle rotation

and finally $OX$ goes into $OX'$. Under these rotations , a new right-handed Cartesian system $OX'Y'Z'$ is formed.

Now, the spherical harmonics $Y_l^m(\hat{r})$, where $\hat{r}$ is the unit vector specifying polar angles with respect to this arbitrary frame, and spin functions $X_s^{m_s}(\eta')$ which are eigen functions of $\sigma_z'$, are written in terms of $Y_l^m(\hat{r})$, $X_s^{m_s}(\eta)$. Where $r$, $\eta$ are spatial and spin coordinates appropriate to the local frame, as

$$Y_l^m(\hat{r}') = \sum_{m'} R^l_{mm'}(\alpha,\beta,\gamma) Y_l^{m'}(\hat{r}) \tag{2.39}$$

$$X_s^{m_s}(\eta') = \sum_{m_s' \pm 1/2} R^{1/2}_{m_s m_s'}(\alpha,\beta,\gamma) X_s^{m_s'}(\eta) \tag{2.40}$$

where

$$R^l_{mm'}(\alpha,\beta,\gamma) = e^{-i\alpha m} r^l_{mm'}(\beta) e^{-i\gamma m'} \qquad (Messiah 1965) \tag{2.41}$$

with the Wigner formula

$$r^l_{mm'}(\beta) = \sum_{t=0} (-1)^t \frac{\sqrt{(l+m)!(l-m)!(l+m')!(l-m')!}}{(l+m-t)!(l-m'-t)!t!(t-m+m')!} \times (\cos\beta/2)^{2l+m-m'} (\sin\beta/2)^{2t-m+m'} \tag{2.42}$$

and

$$R^{1/2}_{m_s m_s'}(\alpha,\beta,\gamma) = \begin{pmatrix} e^{-i\alpha/2}\cos\beta/2 e^{-i\gamma/2} & -e^{-i\alpha/2}\sin\beta/2 e^{i\gamma/2} \\ e^{i\alpha/2}\sin\beta/2 e^{-i\gamma/2} & e^{i\alpha/2}\cos\beta/2 e^{i\gamma/2} \end{pmatrix} \tag{2.43}$$

Now the $t$-matrix, $t^{l,\text{working}}_{m_s,m'm_s'}$ describing scattering from a potential with its magnetic component oriented along $Z$-axis of this arbitrary "working" frame is written in terms of

that of the "local" frame $t^{l,local}_{m_s,m's'}$

$$t^{l,working}_{m_s,m's'} = \sum_{m'',m''',m''_s,m'''_s} R^{l}_{m_s m''_s}(A)(R^{1/2}_{m_s m''_s}(A) t^{l,local}_{m''m''_s,m'''m'''_s} R^{1/2\dagger}_{m'''_s m'_s}(A)) R^{\dagger}_{m'''m'}(A) \quad (2.44)$$

where $A = (\alpha, \beta, \gamma)$ and for the convenience of notation replacing $m_s = \sigma = \pm 1/2$,

$$t^{l,working}_{m\sigma,m'\sigma'} = \sum_{m'',m''',\sigma'',\sigma'''} R^{l}_{mm''}(A)(R^{1/2}_{\sigma\sigma''}(A) t^{l,local}_{m''\sigma'',m'''\sigma'''} R^{1/2\dagger}_{\sigma'''\sigma'}(A)) R^{\dagger}_{m'''m'}(A) \quad (2.45)$$

Non-relativistically, the $t$-matrix satisfies the relation

$$t_{lm\sigma,l'm'\sigma'} = t_{ll'}\delta_{ll'}\delta_{mm'}\delta_{\sigma\sigma'} \quad (2.46)$$

Non-relativistically, the $t$-matrix is dependent only on $l$ through the spherically symmetric potential. But relativistically the $t$-matrix is also dependent on $m$, that is it has different values for different component of $m$ corresponding to a particular $l$, as if a spherically asymmetric potential $V(\underline{r})$ is experienced by the scattering electron. Thus the magnetic anisotropy arises from this $m$ dependence contrary to the non-relativistic case. In order to derive an expression for the interaction between two magnetic impurities in a host lattice, scattering from many potentials needs to be considered. The relevant formalism is outlined in the next section.

## 2.4 Multiple scattering theory

Gyorffy et al (1973) first introduced the powerful scattering path operator $\tau^{ij}$ for multiple scattering problem. This scattering path operator $\tau^{ij}$ gives the scattered waves emanating from the site $\underline{R}_j$ operating on the wave incident at $\underline{R}_i$ and includes all the effects in between. $\sum_{ij} \tau^{ij}$ takes the incident waves arriving at all the sites in the lattice, turns them into scattered waves emanating from all the other sites and adds up all the scattered waves and is thus the total $T$-matrix for the set of scatterers. In the $l, m$ and $\sigma$ representation, the relativistic "on the energy shell" (for non-overlapping potentials) components of the path operator $\tau^{ij}_{lm\sigma,l'm'\sigma'}(E)$ satisfy the following equation (Gyorffy and Stocks 1979)

$$\tau^{ij}_{lm\sigma,l'm'\sigma'} = t^{i,l}_{m\sigma,m'\sigma'}(E)\delta_{ij}\delta_{ll'} + \sum_{k\neq i}\sum_{l'',m'',\sigma'',l''',m'''} t^{i,l}_{m\sigma,m''\sigma''} G^{l''m''}_{l'''m'''}(\underline{R}_i - \underline{R}_k, E)$$
$$\tau^{kj}_{l'''m'''\sigma''',l'm'\sigma'}(E) \quad (2.47)$$

where the structure constants have been written (Staunton et al 1980)

$$G_{lm\sigma,l'm'\sigma'} = G_{lm,l'm'}\delta_{\sigma\sigma'} \tag{2.48}$$

Equation (2.47) is the fundamental equation for multiple scattering on the energy shell and this equation is applicable to non-overlapping, spherically symmetric potentials. This gives $\tau^{ij}_{lm\sigma,l'm'\sigma'}$ in terms of the relativistic spin polarized scattering single site $t$-matrix, $t_{lm\sigma,l'm'\sigma'}$, that is to say in terms of the phase shift and the structure constants. The structure constants $G_{lm,l'm'}(\underline{R}_i - \underline{R}_k; E)$ do not depend on the potential function and are determined by the spatial arrangement of the scattering sites. The scattering path operator matrix $\tau^{ij}_{lm\sigma,l'm'\sigma'}$ is a key parameter in the expression for the interaction between two magnetic impurities derived in chapter 5. In chapter 3, a theory for the energy bands arising from a regular lattice of scattering potentials is presented as an example of the theory of the multiple scattering. The relativistic energy band structure for gold is calculated and a comparison is made with the non-relativistic band structure.

# Chapter 3

# RELATIVISTIC BAND STRUCTURE CALCULATION.

## 3.1 Introduction

For many years, enormous work has been done on energy band structure calculations of metals (e.g. Burdick et al 1963, Takada 1966, Ramchandani 1970). Band structure calculations describe the energy levels of electrons in solids and from the knowledge of these energy levels it can be determined if a material is a conductor or an insulator. If one treats energy eigenvalues of the Kohn-Sham (1965) one particle Schrodinger equation as one-electron eigenvalues as in the one-electron theory of band structure of solids, one can arrive at a band structure of a system via the Density Functional formalism (Callaway et al 1977). From the one-electron energy eigenvalues, one may construct a Fermi surface. Density Functional theory shows that the one-body effective potentials contain all the effects of the electron correlations and the potential is constructed self-consistently. As the KKR (Korringa 1947,Kohn and Rostoker 1954) band structure method is formulated in terms of spherically symmetric non-overlapping muffin-tin potentials, it is appropriate for closed packed cubic systems (e.g fcc, bcc, hcp) and is widely used to study the band structure of metallic systems. This KKR band theory as it stands is inadequate for a

study of the band structure of metals of high atomic number, such as, gold (Z=79). In particular, the relativistic band structure of gold has been investigated by many authors (Ramachandani 1970, Christensen et al 1971, Takeda 1980) by band structure methods generalised to include relativistic effects and a considerable effect of the relativistic spin-orbit interaction is observed for the d-bands. As Au is treated as a host, in this thesis, to study the relativistic interaction between two magnetic impurities (Fe in this thesis), the relativistic band structure of gold is presented in this chapter as a relevant work. In section (3.2), the KKR theory for relativistic band structure is presented. In section (3.3), the results for both the relativistic and non-relativistic band structure for Au are presented and a comparison made.

## 3.2 The relativistic KKR energy band theory

This is based upon the relativistic generalization of the multiple scattering formalism which was described in chapter 2, section 3. Consider a paramagnetic system with an arbitrary arrangement of scattering potentials of the form $v_i(\underline{r}-\underline{R}_i)$ such that the scattering amplitude $t^i$ gives the property of each individual potential scatterer via the phase shift $\delta$ (as discussed in chapter2). Following Staunton et al (1980), in the $\kappa$, $m_j$ representation, the "on the energy shell" components $\tau^{ij}_{\kappa m_j,\kappa' m'_j}(E)$ (see eqn.2.47 in chapter 2) can be written as

$$\tau^{ij}_{\kappa m_j,\kappa' m'_j} = t^i_\kappa(E)\delta_{ij}\delta_{\kappa\kappa'}\delta_{m_j m'_j} + \sum_{n\neq i}\sum_{\kappa'' m''_j} t^i_\kappa(E)G_{\kappa m_j,\kappa'' m''_j}(\underline{R}_i-\underline{R}_n;E)\tau^{nj}_{\kappa'' m''_j,\kappa' m'_j} \qquad (3.1)$$

where $i, j, n$ label the scattering sites at $\underline{R}_i$, $\underline{R}_j$ and $\underline{R}_n$ respectively. $G$ is the relativistic structure constant and it is related to the non-relativistic analogue $G_{lm,l'm'}(\underline{R}_i-\underline{R}_n;E)$ as (Onodera and Okazaki 1966a)

$$G_{\kappa m_j,\kappa' m'_j}(\underline{R}_i-\underline{R}_n;E) = \sum_{\sigma=\pm\frac{1}{2}} C^{\kappa m_j}_{\sigma,m_j-\sigma} G_{lm_j-\sigma,l'm'_j-\sigma}(\underline{R}_i-\underline{R}_n;E) C^{\kappa' m'_j}_{\sigma,m'_j-\sigma} \qquad (3.2)$$

The structure constant describes the free particle propagation from site $i$ to site $n$. The equation (3.1) can only be applied if the potentials are spherically symmetric and non-overlapping. Taking all the scattering potentials to be identical and arranged on a crystal lattice, which is the case for a pure metallic system, so that the scattering amplitudes $t_n^l(E)$ are same, the equation (3.1) can be solved by taking the lattice Fourier transform of both sides and thus

$$\tau^{ij}_{nm_j,n'm'_j}(E) = \frac{1}{\Omega_{BZ}} \int \underline{dk} e^{i\underline{k}.(\underline{R}_i - \underline{R}_j)} \tau_{nm_j,n'm'_j}(\underline{k}, E)$$
$$= \frac{1}{\Omega_{BZ}} \int \underline{dk} [(t^{-1}(E) - G(\underline{k}, E))^{-1}]_{nm_j,n'm'_j} e^{i\underline{k}.(\underline{R}_i - \underline{R}_j)} \qquad (3.3)$$

where $\Omega_{BZ}$ is the volume of the Brillouin zone. $\tau(\underline{k}, E)$ is like a green's function and where it exhibits poles or singularities, the energy eigenvalue spectrum or the energy bands can be found. So, the condition by which the energy eigenvalue spectrum or the energy bands may be determined is

$$\| t^{-1}(E) - G(\underline{k}, E) \|_{nm_j,n'm'_j} = 0 \qquad (3.4)$$

This is the relativistic KKR (Korringa 1947, Kohn and Rostoker 1954) determinant (Staunton et al 1980, Chowdhuri et al 1979, Takada 1966). From (3.3) the site diagonal scattering path operator can also be written

$$\tau^{ii}_{nm_j,n'm'_j} = \frac{1}{\Omega_{BZ}} \int_{BZ} [(t^{-1}(E) - G(\underline{k}, E))^{-1}]_{nm_j,n'm'_j} \underline{dk} \qquad (3.5)$$

The $l$, $m$, and $\sigma$ representation of $\tau^{ij}$ in (3.3) and $\tau^{ii}$ in (3.5) are used for these key quantities in chapter (5) to derive the desired two site interaction. In the $l$, $m$ and $\sigma$ representation (3.3) and (3.5) can simply be written as

$$\tau^{ij}_{lm\sigma,l'm'\sigma'}(E) = \frac{1}{\Omega_{BZ}} \int_{BZ} [(t^{-1}(E) - G(\underline{k}, E))^{-1}]_{lm\sigma,l'm'\sigma'} e^{i\underline{k}.(\underline{R}_i - \underline{R}_j)} \underline{dk} \qquad (3.6)$$

and

$$\tau^{ii}_{lm\sigma,l'm'\sigma'}(E) = \frac{1}{\Omega_{BZ}} \int_{BZ} [(t^{-1}(E) - G(\underline{k}, E))^{-1}]_{lm\sigma,l'm'\sigma'} \underline{dk} \qquad (3.7)$$

The energy band structure for gold is calculated both relativistically and non-relativistically in the next section. For a given energy the wave vector $\underline{k}$ is varied along the high symmetry

points $\Gamma(000)$ to $X(100)$ direction in the irreducible Brillouin zone until equation (3.4) is satisfied. The calculation is repeated for different energies and the wave vectors and the points at which the determinant is zero are sought. In the next section, the result for the relativistic and the non-relativistic band structure of gold is presented only between $\Gamma(000)$ and $X(100)$, the $\Delta$ direction, and the relativistic effect on the band structure of gold is discussed.

## 3.3 Results and discussion

The relativistic band structure of gold is shown fig.(3.1) and for comparison the non-relativistic band structure of gold is also shown in fig.(3.2). The leading relativistic corrections to the Hamiltonian, derived from the Kohn-Sham-Dirac equation for an electron in an electromagnetic field can be written as

$$H = H_{n.r} - \frac{p^4}{8m^3c^2} + \frac{\hbar^2}{4m^2c^2}\frac{1}{r}\frac{dv}{dr}(\underline{s}\,\underline{l}) + \frac{\hbar^2}{8m^2c^2}\nabla^2 v \qquad (Messiah1965) \qquad (3.8)$$

where $H_{n.r}$ is the non-relativistic Hamiltonian and $v$ is the Kohn-Sham one body effective potential. The second term, the mass-velocity term, is the kinetic energy correction term, the third term is the spin-orbit interaction term and the fourth term is the correction term to the effective potential energy, the Darwin term. In fig.(3.1), the mass-velocity and the Darwin terms pull down the energy bands with respect to the non-relativistic energy bands as in fig.3.2. The spin-orbit term has the important effect because this relativistic correction term splits the energy bands. In fig.3.1, the levels at $\Gamma'_{25}$ and $X_5$ (as in fig.3.2) are shown split up into $\Gamma_8^+ + \Gamma_7^+$ and $X_8^+ + X_7^+$ respectively, however, there is no splitting in the non-relativistic result as in fig.3.2. So, the relativistic spin-orbit correction term has a great influence on the band structure of a system of high atomic number, say for Au (Z=79). The effects of the relativistic band structure of the host will show up in the interaction between the two magnetic impurities. In the next chapter, the non-relativistic and the relativistic RKKY interaction (Staunton et al 1988), in terms of this scattering theory language, are discussed.

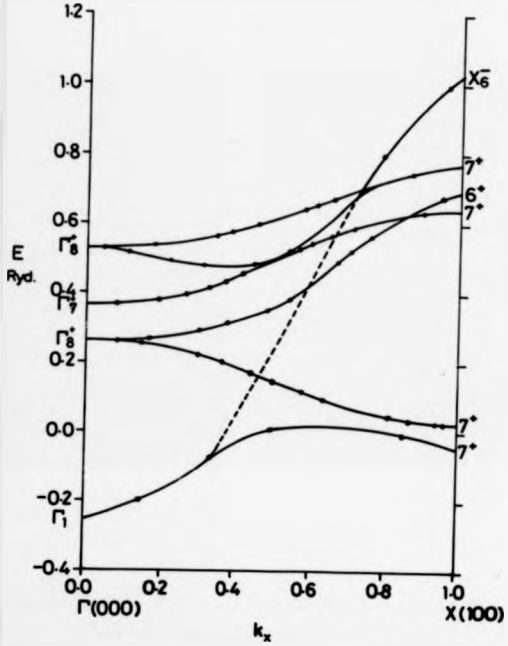


Figure 3.1: Relativistic band structure for gold calculated using muffin-tin potential constructed from the overlapping atomic charge density (Ginatempo).

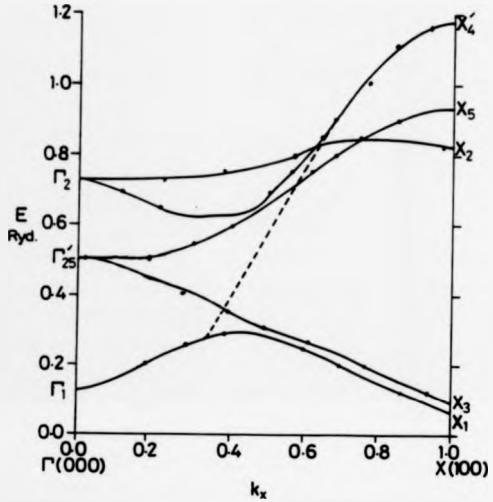


Figure 3.2: Non-relativistic band structure for gold calculated using muffin-tin potential constructed from the overlapping atomic charge density (Ginatempo).

# Chapter 4

# Interaction between two magnetic atoms embedded in a jellium model background

Many authors have derived theories of anisotropic exchange interaction between two magnetic atoms by incorporating the spin-orbit coupling in the Heisenberg direct exchange as a perturbation. Most of them derived the symmetric pseudo-dipolar interaction (Moriya et al 1953, Nagamiya et al 1955). The terms derived by Dzyaloshinsky (1958) and Moriya (1960) are antisymmetric in nature (D.M. terms). Recently Goldberg et al (1986) derived an interaction between two magnetic impurities, which contains the anisotropic effect in an antisymmetric D.M. type term, by considering the spin-orbit scattering between the two magnetic impurity spins via a third non-magnetic site. Staunton et al (1988) derived an interaction between two magnetic impurities in a uniform potential background (relativistic jellium model) in which the anisotropic effect was shown as a polynomial dependence upon both the pseudo-dipolar term and the squared D.M. term (hence symmetric), set up by a relativistic electron scattering between them.

In this chapter, the relativistic RKKY interaction and the anisotropic effect for two Fe impurities studied by Staunton et al (1988) are summarised and its non-relativistic limit,

the RKKY interaction, is also discussed.

Using the local density approximation (Kohn et al 1965, Kohn and Vashista 1982) for the exchange and correlations contributions, the Grand potential $\Omega$ of a system of interacting electrons at a temperature T within the relativistic and spin-density functional formalism (Gunnarsson 1976, MacDonald et al 1979, Rajagopal 1980) is written as

$$\Omega[n,\underline{m}] = \int dE.E.n(E)f(E-\nu) - \frac{e^2}{2}\int\int \underline{dr}\underline{dr'}\frac{n(\underline{r})n(\underline{r'})}{|\underline{r}-\underline{r'}|}$$
$$-\int \underline{dr}|\frac{\delta E^R_{xc}}{\delta n(\underline{r})}n(\underline{r}) + \frac{\delta E^R_{xc}}{\delta \underline{m}}.\underline{m}(\underline{r})| + \int \epsilon^R_{xc}(n(\underline{r}))n(\underline{r})\underline{dr} \qquad (4.1)$$

where $n(E)$ is the density of states, $f(E-\nu)$ is the Fermi-Dirac function, $\nu$ is the chemical potential, $E^R_{xc}$ is the relativistic exchange and correlation energy of an interacting system with electron density $n(\underline{r})$ and magnetization density $\underline{m}(\underline{r})$ and $\epsilon^R_{xc}$ is the exchange and correlation energy per electron of a uniform electron gas.

If $\nu$, n and the magnitude of the magnetization density, $|\ \underline{m}\ |$, are unchanged as the direction of the magnetization of the system is varied, the magnetic anisotropic effect is contained in the first "single particle" energy term. Recalling the first term

$$\int_0^\infty dE.E.n(E)f(E-\nu) = \nu Z - \int_0^\infty f(E-\nu)N(E)dE \qquad (4.2)$$

where $N(E)$ is the integrated density of states and Z is the number of electrons per atom. The magnetic anisotropic effect is contained in the second term

$$\Omega' = -\int_0^\infty f(E-\nu)N(E)dE \qquad (4.3)$$

The integrated density of states for two atoms in a jellium model is (Lloyd and Smith 1972)(suppressing the l, m and $\sigma$ representation)

$$N(E) = N_o - \frac{Im}{\pi}tr\ln(t^{-1}_{m1,2} - G)$$
$$= N_o - \frac{Im}{\pi}\ln|\ t_1^{-1}\ | - \frac{Im}{\pi}\ln|\ t_2^{-1}\ | - \frac{Im}{\pi}\ln|\ 1 - t_1G_{12}t_2G_{21}\ | \qquad (4.4)$$

where $N_o$ is the integrated density of states for free electron and $G_{12} = G_{lm,l'm'}(\underline{R}_1 - \underline{R}_2, E)$ is the structure constant and is defined as (Lloyd and Smith 1972)

$$G_{lm,l'm'}(\underline{R}_{12}, E) = 4\pi\sqrt{E}\sum_{l''m''} i^{l''}C^{l''m''}_{lm,l'm'}Y^{m''}_{l''}(\underline{\hat{R}}_{12})h^1_{l''}(R_{12}, E) \qquad (4.5)$$

where $h_l^1$ is the Hankel function, the spherical harmonics $Y_l^m$ set up the Gaunt numbers

$$C_{lm,l'm'}^{l''m''} = \int Y_l^m(\hat{r}) Y_{l'm''}^{m''}(\hat{r}) Y_{l'}^{m'}(\hat{r}) d\hat{r} \tag{4.6}$$

with $m'' = m' - m$, $(l + l' + l'')$ even and $|\ l' - l\ | \leq l'' \leq (l + l')$ (Lloyd and smith 1972). For two well separated sites, using the fourth term in expression (4.4), Staunton et al (1988) derived the relativistic generalisation for the interaction between the two magnetic impurities $t^1$, $t^2$ as

$$\Omega_{12} = \frac{Im}{\pi} \int dE f(E - \nu) \sum_{l_3 m_3 \sigma_3 l_4 m_4 \sigma_4} t^1_{l_1 m_1 \sigma_1, l_3 m_3 \sigma_3}$$
$$G_{l_3 m_3, l_4 m_4}(R_{12}, E) t^2_{l_3 m_3 \sigma_3, l_4 m_4 \sigma_4} G_{l_4 m_4, l_1 m_1}(R_{12}, E) \tag{4.7}$$

In the non-relativistic limit the single site $t$-matrix with "spin" $\hat{S}$ along an arbitrary direction $\hat{e}$ is

$$t = t_1 \bar{1} + \underline{e} . \hat{e} t_2 \tag{4.8}$$

where $\sigma$ represents the Pauli matrices. If the spin is along Z-axis i.e. $\hat{e} - Z$

$$t = t_1 \bar{1} + \sigma_Z t_2 = \begin{pmatrix} t_1 + t_2 & 0 \\ 0 & t_1 - t_2 \end{pmatrix}$$
$$= \begin{pmatrix} t_{1/2} & 0 \\ 0 & t_{-1/2} \end{pmatrix} \tag{4.9}$$

where $t_1 = \frac{1}{2}(t_{1/2} + t_{1/2})$ and $t_2 = \frac{1}{2}(t_{1/2} - t_{-1/2})$ and $t_\sigma = t_{lm\sigma, l'm'\sigma'} = t^{lm}_{\sigma\sigma'} \delta_{mm'} \delta_{ss'} \delta_{ll'}$. where the superscript '1' represents a particular impurity scatterer. Because the structure factor G is independent of $\sigma$ and $\hat{S}$, the $t$-matrices for the two impurity spins oriented along $\hat{S}_1$ and $\hat{S}_2$ can be written together

$$\Omega^{(2)1} = tr t^{1,l_1} t^{2,l_2} G(R_{12}, E) G(R_{21}, E)$$
$$= tr[t_1^{1,l_1} t_1^{2,l_2} + t_2^{1,l_1} t_2^{2,l_2} \underline{\sigma} . \hat{S}_1 \underline{\sigma} . \hat{S}_2] GG$$
$$= tr[\frac{1}{4}(t^{1,l_1}_{1/2} + t^{1,l_1}_{-1/2})(t^{2,l_2}_{1/2} + t^{2,l_2}_{-1/2}) + \frac{1}{4}(t^{1,l_1}_{1/2} - t^{1,l_1}_{-1/2})(t^{2,l_2}_{1/2} - t^{2,l_2}_{-1/2}) \hat{S}_1 . \hat{S}_2] GG \tag{4.10}$$

Therefore, the non-relativistic interaction between the two magnetic atoms is

$$E_{12} = \frac{Im}{\pi} \int dE f(E - \nu) \sum_{l_1 l_2} (\frac{1}{4}(t^{1,l_1}_{\frac{1}{2}\frac{1}{2}} + t^{1,l_1}_{-\frac{1}{2}-\frac{1}{2}})(t^{2,l_2}_{\frac{1}{2}\frac{1}{2}} + t^{2,l_2}_{-\frac{1}{2}-\frac{1}{2}})$$

$$+\frac{1}{4}(t^{1,l_1}_{\frac{1}{2}\frac{1}{2}} - t^{1,l_1}_{-\frac{1}{2}-\frac{1}{2}})(t^{2,l_2}_{\frac{1}{2}\frac{1}{2}} - t^{2,l_2}_{-\frac{1}{2}-\frac{1}{2}})\hat{S}_1.\hat{S}_2) \sum_{m_1 m_2} G_{l_1 m_1, l_2 m_2}(\underline{R}_{12}, E) G_{l_2 m_2, l_1 m_1}(\underline{R}_{21}, E) \quad (4.11)$$

The dependence of the interaction on the direction of $\underline{R}_{12}$ vanishes through trigonometrical relations as the summation over $m_1$ and $m_2$ is carried out and the second sum is only proportional to

$$E i^{(l''+l''')} h^{\dagger}_{l''}(\sqrt{E}R_{12}) h^{\dagger}_{l'''}(\sqrt{E}R_{12}) \quad (4.12)$$

Since the $t$-matrices depend only weakly upon energy, this term contains the dominant interaction energy between the two impurity spins. So, taking the asymptotic limit of the Hankel function $h^{\dagger}_0(\sqrt{E}R_{12}) \xrightarrow{R_{12}\to\infty} \frac{-i}{\sqrt{E}R_{12}} e^{i\sqrt{E}R_{12}}$, the interaction between the two impurity spins embedded in a jellium model is proportional to

$$E_{12} \propto \frac{Im}{\pi} \int_0^{k_F} k^2.2k.dk. \frac{e^{2ikR_{12}}}{k^2 R^4_{12}}$$

$$= \frac{1}{2\pi R^4_{12}} [2k_F R_{12} \cos 2k_F R_{12} - \sin 2k_F R_{12}] \quad (4.13)$$

which is of the standard RKKY form.

Staunton et al (1988) expressed their relativistic interaction between the two magnetic impurities (eqn.4.7) as

$$E_{12} = \sum_{i=0}^{2l_{max.}} \sum_{j=0}^{2l_{max.}} a_{ij} (\hat{S}_1.\hat{S}_2)[(\hat{R}_{12}.\hat{S}_1)(\hat{R}_{12}.\hat{S}_2)]^i [\hat{R}_{12}.(\hat{S}_1 \times \hat{S}_2)]^{2j} \quad (4.14)$$

where the coefficients $a_{ij}$ depend on the relative orientations of the spins on sites 1 and 2 through the $t$-matrices for each sites. $l_{max.}$ is the maximum orbital angular momentum for which the scattering is significant. In this expression, the anisotropic effect is very obvious through the polynomial function of pseudo-dipolar term and the squared D.M. terms. For transition metals $l_{max.} = 2$. In the fig.(4.1), the relativistic RKKY interaction and its anisotropic components are presented for two Fe impurities (Staunton et al 1988). In this it is discovered that along with the oscillatory relativistic RKKY interaction, the anisotropic component is also oscillatory as a function of separation. In the next chapter, the desired relativistic interaction between the two impurities in a realistic host is derived.

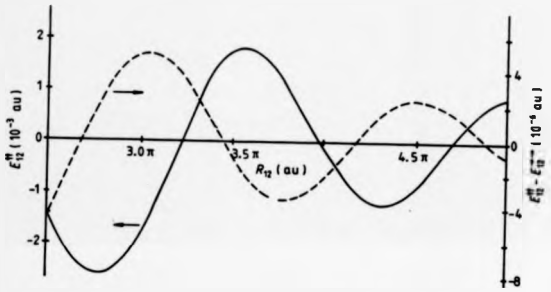


Figure 4.1: The relativistic RKKY interaction ($E_{12}^{\perp\perp}$) and its anisotropic component ($E_{12}^{\perp\perp} - E_{12}^{\rightarrow\rightarrow}$) as a function of separation (Staunton et al 1988). $E_{12}^{\perp\perp}$ is the interaction energy for both impurity spins perpendicular to the separation vector $\underline{R}_{12}$ and $E_{12}^{\rightarrow\rightarrow}$ is the interaction energy for both impurity spins parallel to the separation vector $\underline{R}_{12}$.

# Chapter 5

# THEORY FOR THE ANISOTROPIC INTERACTION BETWEEN TWO MAGNETIC IMPURITIES IN A REALISTIC HOST

## 5.1 Introduction

Some theories for studying dilute alloys are developed on the assumption of a single impurity in metals and the interaction effects between the impurities are considered to be negligible. As a first approach, the Friedel sum rule and the Friedel oscillations of the charge density (Friedel 1958) around an impurity for a dilute alloy are deduced within an elementary scattering theory framework. In recent years, substantial progress has been made in the study of dilute alloys by the development of the density functional theory. Stefanou et al (1987) reported a self-consistent calculation introducing the KKR Green's function method and calculated the charge and magnetization perturbation (Friedel os-

cillation type) around an impurity atom in a dilute Ni-host. Dederich et al (1987) used this same formalism to study the electronic structure of dilute alloys of transition metal impurities in noble metals (Cu, Au). The interaction between two impurities is important in studying spin-glass and magnetic properties of dilute alloys. Alloy problems are usually studied with the assumption that the impurities are substitutional for atoms of the host lattice. Temmerman (1982) first reported a formalism for studying the non-relativistic interaction between two substitutional impurities in a realistic host within a scattering theory framework. In the following year,Oguchi et al (1983) first applied this non-relativistic two site interaction to study magnetism of iron at high temperatures. In this chapter, a relativistically based interaction between two impurities in a crystalline host is derived. Firstly, an expression for the relativistically generalized number of states due to two substitutional impurities (1 and 2) described by $t_1^i$ and $t_2^i$ in a pure metallic host is derived in section (5.2). The number of states, which is relativistically generalized, for a pure metallic host is subtracted from the number of states of that system with two substitutional impurities and thereby, an expression for the relativistic interaction between two substitutional magnetic impurities in a realistic paramagnetic host (e.g. Au, Cu etc.) is achieved.

In section (5.3), a convenient "working" coordinate frame is specified with respect to the axes of the fcc (Au or Cu host) crystal axes. Quantities (say $t$-matrices) expressed in "local" coordinate frames (i.e. the frame with its Z-axis set up along the magnetic component of the impurity potential) can be written in terms of the "working" frame by considering the usual Euler angles of rotation (see fig.5.2). An outline of how the relativistic interaction between two magnetic impurities and its anisotropic component are studied by rotating the magnetic components on the two impurities in various orientations and which is shown in detail in the following chapter, is also presented at the end.

## 5.2 Relativistic interaction between two magnetic impurities in a metallic host

As earlier mentioned (eqn.4.3) in chapter 4, the relativistic interaction energy between two magnetic impurities and the anisotropic effect are contained in the expression

$$\Omega' = -\int_0^{\infty} f(E-\nu)N(E)dE \tag{5.1}$$

where N(E) is the integrated density of states induced by two magnetic impurities in a metallic host. The relativistically generalized integrated density of states of a pure system is (Lloyd and Smith 1972, Gyorffy and Stocks 1979)

$$N(E) = N_o(E) - \frac{1}{\pi} Im \ln \| t^{o-1}_{n,\Lambda\Lambda'}(E)\delta_{nn'} - G^o_{\Lambda\Lambda'}(\underline{R}_n - \underline{R}_{n'}, E)\delta_{\sigma\sigma'} \| \tag{5.2}$$

where $N_o(E)$ is the free electron integrated density of states and $\Lambda = (l, m, \sigma)$. $t^{-1}$ is the inverse of the relativistic transition matrix for the scattering sites and $G^o$ is the structure factor matrix. The second term of equation (5.2) arises from the multiple scattering effect. For convenience, for the time being the angular momentum and spin indices for the matrices will be suppressed.

Focussing on the second term of eqn.(5.2), using $tr(\bar{M}) = det \mid \bar{M} \mid$ for the site index part of the matrices, the relativistically generalized number of states due to the scattering sites of the host system containing the two substitutional impurities (see fig.5.1) is written

$$N_1 = -\frac{1}{\pi} Im \ln \left| \left( \begin{array}{cc} t^{I-1}_{n=1,2} & 0 \\ 0 & t^{o-1}_{n\neq 1,2} \end{array} \right) + \left( \begin{array}{cc} 0 & -G^o \\ -\bar{G}^o & 0 \end{array} \right) \right| \tag{5.3}$$

The $t$-matrices in this expression is expressed in "working" frame i.e. rotated through Euler angles. The trace operation on the angular momentum and spin indices (i.e. $\Lambda = l, m, \sigma$) has yet to be carried out. In expression (5.3) $t^{I-1}_{n=1,2}$ is a $2 \times 2$ diagonal matrix for the two impurity sites, $t^{o-1}_{n\neq 1,2}$ is a $(N-2) \times (N-2)$ diagonal matrix for the $(N-2)$ host sites, $G^o$ and $\bar{G}^o$ are off diagonal $2 \times 2$ and $(N-2) \times (N-2)$ matrices respectively consisting only of the real space structure constants (Lloyd and smith 1972). The superscript "$I$"

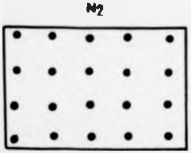


Figure 5.1(a): Host system


Figure 5.1(b): Host system with two impurities.

and "$O$" refer to the impurity and the host sites respectively, $n$ denotes a particular site and $N$ is for the total number of sites.

The relativistically generalized induced number of states due to two substitutional impurities in a paramagnetic host

$$\Delta N(E) = N_1(E) - N_2(E)$$

$$= -\frac{1}{\pi} Im \ln \left| \begin{pmatrix} t^{I^{-1}}_{n=1,2} & 0 \\ 0 & t^{o^{-1}}_{n\neq 1,2} \end{pmatrix} + \begin{pmatrix} 0 & -G^{o} \\ -\tilde{G}^{o} & 0 \end{pmatrix} \right|$$

$$+ \frac{1}{\pi} Im \ln \left| \begin{pmatrix} t^{o^{-1}}_{n=1,2} & 0 \\ 0 & t^{o^{-1}}_{n\neq 1,2} \end{pmatrix} + \begin{pmatrix} 0 & -G^{o} \\ -\tilde{G}^{o} & 0 \end{pmatrix} \right|$$

$$= -\frac{1}{\pi} Im \ln \left| \begin{pmatrix} t^{o^{-1}}_{n=1,2} & 0 \\ 0 & t^{o^{-1}}_{n\neq 1,2} \end{pmatrix} + \begin{pmatrix} (t^{I^{-1}}_{n} - t^{o^{-1}}_{n})_{n,n'=1,2}\delta_{nn'} & 0 \\ 0 & 0 \end{pmatrix} + \begin{pmatrix} 0 & -G^{o} \\ -G^{o} & 0 \end{pmatrix} \right|$$

$$+ \frac{1}{\pi} Im \ln \left| \begin{pmatrix} t^{o^{-1}}_{n=1,2} & 0 \\ 0 & t^{o^{-1}}_{n\neq 1,2} \end{pmatrix} + \begin{pmatrix} 0 & -G^{o} \\ -\tilde{G}^{o} & 0 \end{pmatrix} \right| \quad (5.4)$$

Using the relation, which is relativistically generalized, (Gyorffy and Stott 1973, Staunton et al 1980)

$$(\tau^{-1})^{nn'}_{\Lambda\Lambda'} = t^{o^{-1}}_{n,\Lambda\Lambda'}\delta_{nn'} - G_{\Lambda\Lambda'}(R_n - R_{n'}, E)\delta_{\sigma\sigma'} \quad (5.5)$$

where $G^{n}_{lm,l'm'}(R_n - R_{n'}) = 4\pi\sqrt{E}\sum_{l''m''} i^{l''} C^{l''m''}_{lm,l'm'} Y^{m''}_{l''}(\hat{R}_{nn'}) h^{+}_{l''}(R_{nn'}, E)$ and

$$\Delta N(E) = -\frac{1}{\pi} Im \ln(|| \tau^{-1} + \Delta_{n,n'=1,2}\delta_{nn'} ||) + \frac{1}{\pi} Im \ln(|| \tau^{-1} ||) \quad (5.6)$$

where $\tau^{nn'}_{\Lambda\Lambda'}$, the path operator matrix element, introduced by Gyorffy and Stott (1973) is relativistically generalized in this case. As described in chapter 3, $\tau$ describes the energy bands of the pure host system, its poles determine the energy eigenvalues. The realistic host effect can be contained in the desired two site interaction through this path operator matrix $\tau$. In the expression (5.6)

$$\Delta_{n,n'=1,2}\delta_{nn'} = \begin{pmatrix} t_1^{-1} - t_1^{o^{-1}} & 0 & 0 & 0 & 0 & 0 \\ 0 & t_2^{-1} - t_2^{o^{-1}} & 0 & 0 & 0 & 0 \\ 0 & 0 & 0 & 0 & 0 & 0 \\ 0 & 0 & 0 & 0 & 0 & 0 \\ 0 & 0 & 0 & 0 & 0 & 0 \\ 0 & 0 & 0 & 0 & 0 & 0 \end{pmatrix} = \begin{pmatrix} \Delta_1 & 0 & 0 & 0 \\ 0 & \Delta_2 & 0 & 0 \\ 0 & 0 & 0 & 0 \\ 0 & 0 & 0 & 0 \end{pmatrix} \equiv \Delta_{1,2} \tag{5.7}$$

Now

$$\Delta N(E) = -\frac{1}{\pi} Im \ln(\| \tau^{-1} \|) - \frac{1}{\pi} Im \ln(\| 1 + \tau\Delta_{1,2} \|) + \frac{1}{\pi} Im \ln(\| \tau^{-1} \|)$$

$$= -\frac{1}{\pi} Im \ln(\| 1 + \tau\Delta_{1,2} \|) = -\frac{1}{\pi} Im \ln(\| 1 + \tau^{11}\Delta_1 \|) - \frac{1}{\pi} Im \ln(\| 1 + \tau^{22}\Delta_2 \|)$$

$$-\frac{1}{\pi} Im \ln \left| 1 + \begin{pmatrix} 0 & (1+\tau^{11}\Delta_1)^{-1}\tau^{12}\Delta_2 & 0 & 0 \\ (1+\tau^{22}\Delta_2)^{-1}\tau^{21}\Delta_1 & 0 & 0 & 0 \\ 0 & 0 & 0 & 0 \\ 0 & 0 & 0 & 0 \end{pmatrix} \right| \tag{5.8}$$

The first and the second terms are the relativistic induced number of states for the individual impurity sites 1 and 2 respectively. The third term is the net induced number of states due to the interaction between the impurity sites via the host.

Therefore, the relativistic induced number of states due to the interaction between two impurities in a realistic metallic host

$$N(E) = -\frac{1}{\pi} Im \ln \begin{vmatrix} 1 & (1+\tau^{11}\Delta_1)^{-1}\tau^{12}\Delta_2 & 0 & 0 \\ (1+\tau^{22}\Delta_2)^{-1}\tau^{21}\Delta_1 & 1 & 0 & 0 \\ 0 & 0 & 1 & 0 \\ 0 & 0 & 0 & \bar{1} \end{vmatrix}$$

$$= -\frac{1}{\pi} Im \ln(\bar{1} - (1 + \tau^{11}\Delta_1)^{-1}\tau^{12}\Delta_2(1 + \tau^{22}\Delta_2)^{-1}\tau^{21}\Delta_1) \qquad (5.9)$$

Because $\tau^{12} \sim \frac{1}{R_{12}}$, expanding the natural logarithm and retaining the first term for two well separated impurity sites

$$N(E) \simeq \frac{1}{\pi} Im \sum_{lms} (1 + \tau^{11}\Delta_1)^{-1}\tau^{12}\Delta_2(1 + \tau^{22}\Delta_2)^{-1}\tau^{21}\Delta_1)_{lms,lms}$$

$$= \frac{1}{\pi} Im \sum_{lms} (\bar{M})_{lms,lms} \qquad (5.10)$$

Here, the trace operation over the angular momentum and spin has been re-introduced. Now, the relativistic interaction between two magnetic impurities in a paramagnetic host is

$$E_{12} = \frac{1}{\pi} Im \int_0^\infty dE f(E - \nu) \sum_{\Lambda} (\bar{M})_{\Lambda\Lambda} \qquad (5.11)$$

This is the key expression which is used to calculate the anisotropic interaction energy between two impurity sites. This can be reduced to the interaction energy between two magnetic impurities embedded in a jellium model for both relativistic and non-relativistic cases [Appendix A].

The matrix element of $\bar{M}$ labelled by the orbital, the magnetic and the spin quantum numbers, which is the case of the relativistic generalization, is

$$(\bar{M})_{\Lambda,\Lambda'} = \sum_{\Lambda_1,\Lambda_2,\Lambda_3,\Lambda_4,\Lambda_5} M^1_{\Lambda,\Lambda_1}\tau^{12}_{\Lambda_1,\Lambda_2}\Delta_{2,\Lambda_2,\Lambda_3} M^2_{\Lambda_3,\Lambda_4}\tau^{21}_{\Lambda_4,\Lambda_5}\Delta_{1,\Lambda_5,\Lambda'}$$

$$M^1_{\Lambda,\Lambda_1} = [(\bar{1} + \tau^{11}\Delta_1)^{-1}]_{\Lambda,\Lambda_1} = [\bar{N}_1^{-1}]_{\Lambda,\Lambda_1}$$

$$\text{and} \qquad M^2_{\Lambda,\Lambda_1} = [(\bar{1} + \tau^{22}\Delta_2)^{-1}]_{\Lambda,\Lambda_1} = [\bar{N}_2^{-1}]_{\Lambda,\Lambda_1} \qquad (5.12)$$

where the matrix elements for $\bar{N}_1$ and $\bar{N}_2$ are

$N_{1,\Lambda_1,\Lambda_2} = (\delta_{\Lambda_1\Lambda_2} + \sum_{\Lambda'} \tau^{11}_{\Lambda_1\Lambda'}\Delta_{1,\Lambda',\Lambda_2})$

and $N_{2,\Lambda_1,\Lambda_2} = (\delta_{\Lambda_1\Lambda_2} + \sum_{\Lambda'} \tau^{12}_{\Lambda_1,\Lambda'}\Delta_{1,\Lambda',\Lambda_2})$

So, for two well separated magnetic impurities, the relativistic interaction energy between two magnetic impurities in a paramagnetic host is

$$E_{12} \simeq \frac{1}{\pi} Im \int_0^\infty dE f(E - \nu) \sum_{\Lambda_1,\Lambda_2,\Lambda_3,\Lambda_4,\Lambda_5} M^1_{\Lambda\Lambda_1}\tau^{12}_{\Lambda_1\Lambda_2}\Delta_{2\,\Lambda_2\Lambda_3} M^2_{\Lambda_3\Lambda_4}\tau^{21}_{\Lambda_4\Lambda_5}\Delta_{1,\Lambda_5\Lambda} \qquad (5.13)$$

where $\Lambda, \Lambda_1 \ldots\ldots = lm\sigma, l_1 m_1 \sigma_1 \ldots\ldots$ For a pure metallic host

$$\tau^{11}_{\Lambda_1\Lambda_2}(E) = \frac{1}{\Omega_{BZ}} \int_{BZ} d\underline{k} ((t^{o^{-1}} - G^o(\underline{k}, E)^{-1})_{\Lambda_1\Lambda_2} \tag{5.14}$$

$$\tau^{12}_{\Lambda_1\Lambda_2}(E) = \frac{1}{\Omega_{BZ}} \int_{BZ} d\underline{k} ((t^{o^{-1}} - G^o(\underline{k}, E))^{-1})_{\Lambda_1\Lambda_2} e^{i\underline{k}\cdot\underline{R}_{12}} \tag{5.15}$$

where $G^o(\underline{k}, E)$ is the lattice fourier transform of $G^o(\underline{R}_{12}, E)$ and $\Omega_{BZ}$ is Brillouin zone volume. A substantial computational task is involved in the calculation of (5.14) and (5.15). Equation (5.13) is to be calculated in a working frame to calculate the relativistic two site interactions and the anisotropic component. In the next section, details about the convenient working frame are presented.

## 5.3 A convenient working frame

In this section, a convenient working frame is set up with its three axes (X,Y,Z) oriented along the crystal axes (a,b,c) of the fcc (Au or Cu) cubic host system. Of course, the interaction between the two impurities in the host is independent of the choice of the coordinate frame. In equation (5.13) the quantities evaluated in "local" frames are expressed via Euler angles in terms of this "working" frame i.e. $t^{I^{-1}}$. The local frames at 1 and 2 are defined by the requirement that their Z-axes are oriented along the directions $\hat{S}_1$ and $\hat{S}_2$ of the magnetic moments of the two impurities (Fig.5.2). In fig.(5.2) $(X, Y, Z)$ are the axes of the convenient "working" frame at two impurity sites 1 and 2, set up by rotating the axes of the "local" coordinate frame through Euler angles $A_1(\alpha_1, \beta_1, \gamma_1)$ at impurity site 1 and $A_2(\alpha_2, \beta_2, \gamma_2)$ at impurity site 2.

In equation (5.13), in the working frame,

$$\Delta_{1,\Lambda\Lambda_1} = (R^\dagger t_1^{I^{-1}} R - t_1^{o^{-1}})_{\Lambda\Lambda_1}$$

$$\text{and} \qquad \Delta_{2,\Lambda\Lambda_1} = (R^\dagger t_2^{I^{-1}} R - t_2^{o^{-1}})_{\Lambda\Lambda_1} \tag{5.16}$$

The matrix property $(R^\dagger t R)^{-1} = R^\dagger t^{-1} R$ is used in here. Now in (5.16) the inverse of the $t$-matrix, $(t^{-1})_{lm\sigma,l'm'\sigma'}$ which describes scattering from a potential with its magnetic

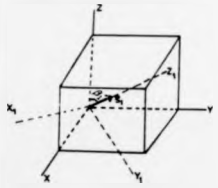

Figure 5.2(a): Working frame and local frame at impurity site 1.

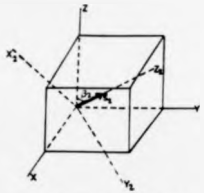

Figure 5.2(b) Working frame and local frame at impurity site 2.

part oriented along some arbitrary direction with respect to the $Z$-axis of the convenient "working" frame can be written in terms of that in the "local" frame, $(t^{-1})_{lm\sigma,l'm'\sigma'}$

$$(t^{-1})_{lm\sigma,l'm'\sigma'} = \sum_{m'',m''',\sigma'',\sigma'''} R^{\frac{1}{2}\dagger}_{m\sigma m''\sigma''}(A)[R^{\frac{1}{2}\dagger}_{\sigma''\sigma'''}(A)(t^{-1})_{lm''\sigma''l'm'''\sigma'''}R^{\frac{1}{2}}_{\sigma'''\sigma'}(A)]R^{\ell}_{m'''m'}(A) \tag{5.17}$$

The Euler angles have to be calculated using the Euler angle rotation operator. The Euler angle rotation operator, which can transform the "working" frame into some other coordinate frame like the "local" frame is (Messiah 1965)

$$R(\alpha,\beta,\gamma) = \begin{pmatrix} \cos\gamma\cos\beta\cos\alpha - \sin\gamma\sin\alpha & -\sin\gamma\cos\beta\cos\alpha - \cos\gamma\sin\alpha & \sin\beta\cos\alpha \\ \cos\gamma\cos\beta\sin\alpha - \sin\gamma\cos\alpha & -\sin\gamma\cos\beta\sin\alpha + \cos\gamma\cos\alpha & \sin\beta\sin\alpha \\ -\cos\gamma\sin\beta & \sin\gamma\sin\beta & \cos\beta \end{pmatrix} \tag{5.18}$$

Throughout the whole calculation $\alpha$ is kept zero. For site 1, the unit vectors along the axes of the convenient "working" frame $(\hat{X},\hat{Y},\hat{Z})$ can be transformed into the unit vectors of the local frame $(\hat{X}_1,\hat{Y}_1,\hat{Z}_1)$ by

$$\begin{pmatrix} \hat{X}_1 \\ \hat{Y}_1 \\ \hat{Z}_1 \end{pmatrix} = R(\alpha,\beta,\gamma) \begin{pmatrix} \hat{X} \\ \hat{Y} \\ \hat{Z} \end{pmatrix} \tag{5.19}$$

Thus

$$\hat{X}_1 = (\cos\gamma_1\cos\beta_1\cos\alpha_1 - \sin\gamma_1\sin\alpha_1)\hat{X} + (-\sin\gamma_1\cos\beta_1\cos\alpha_1 - \cos\gamma_1\sin\alpha_1)\hat{Y} + (\sin\beta_1\cos\alpha_1)\hat{Z}$$

$$\hat{Y}_1 = (\cos\gamma_1\cos\beta_1\sin\alpha_1 + \sin\gamma_1\cos\alpha_1)\hat{X} + (-\sin\gamma_1\cos\beta_1\sin\alpha_1 + \cos\gamma_1\cos\alpha_1)\hat{Y} + (\sin\beta_1\sin\alpha_1)\hat{Z}$$

$$\hat{Z}_1 = (-\cos\gamma_1\sin\beta_1)\hat{X} + (\sin\gamma_1\sin\beta_1)\hat{Y} + (\cos\beta_1)\hat{Z} \quad (5.20)$$

Therefore, for site 1,

$$\begin{aligned} Z_1.\hat{X} &= \hat{S}_1.\hat{X} = -\cos\gamma_1\sin\beta_1 \\ Z_1.\hat{Y} &= \hat{S}_1.\hat{Y} = \sin\gamma_1\sin\beta_1 \\ \hat{Z}_1.\hat{Z} &= \hat{S}_1.\hat{Z} = \cos\beta_1 \end{aligned} \quad (5.21)$$

where $Z_1 = \hat{S}_1$ is the unit vector along the magnetic component of the impurity potential at site 1.

Similarly, for site 2

$$\begin{aligned} \hat{Z}_2.\hat{X} &= \hat{S}_2.\hat{X} = -\cos\gamma_2\sin\beta_2 \\ Z_2.\hat{Y} &= \hat{S}_2.Y = \sin\gamma_2\sin\beta_2 \\ \hat{Z}_2.\hat{Z} &= \hat{S}_2.\hat{Z} = \cos\beta_2 \end{aligned} \quad (5.22)$$

where $\hat{Z}_2 = \hat{S}_2$ is the unit vector along the magnetic component of the impurity potential at site 2. Using equations (5.21)and(5.22), the two spins can be oriented in various desired directions in the "working" frame. The angle between the two spins is

$$\hat{S}_1.\hat{S}_2 = \cos\gamma_1\sin\beta_1\cos\gamma_2\sin\beta_2 + \sin\gamma_1\sin\beta_1\sin\gamma_2\sin\beta_2 + \cos\beta_1\cos\beta_2 \quad (5.23)$$

$\beta$ and $\gamma$ are restricted by $0 \leq \beta \leq \pi$, $-\pi \leq \gamma \leq +\pi$. In the convenient working frame, for some arbitrary orientation of the two impurity spins, the relativistic interaction between two magnetic impurities in a realistic host is

$$E_{12} \simeq \frac{1}{\pi} Im \int dE f(E-\nu) \sum_{A_1 A_2 A_3 A_4 A_5} M^1_{\Lambda\Lambda_1} \tau^{12}_{A_1 A_2} \Delta_{2.A_2 A_3}(\alpha_2,\beta_2,\gamma_2) M^2_{A_3 A_4} \tau^{21}_{A_4 A_5} \times \Delta_{1.A_5 A}(\alpha_1,\beta_1,\gamma_1) \quad (5.24)$$

The next stage of this thesis is to describe how to compute this equation for various orientations of the spin components on the impurity sites 1 and 2 in the "working" frame. The $t$-matrix is calculated using the computational technique discussed in the second section of chapter (2) and the inverse of that is taken. The inverse of the $t$-matrices for the impurity sites (1 and 2), calculated in their "local" frames, are expressed in terms of the working frame using equation (5.17) through the Euler angles. In the next chapter, details about the computational procedure of $\tau$-matrices and finally the integration involved in equation (5.24) are presented.

# Chapter 6

# TWO Fe IMPURITIES IN A NOBLE METAL

## 6.1 Introduction

The most time consuming part of the work described by this thesis has been spent in to computing the key equation (5.24). It describes the interaction between two Fe impurities, orientating their spin components in various directions with reference to a convenient "working" frame associated with the lattice vectors of the fcc Au and Cu hosts. Firstly, the matrices $\tau^{11}$ and $\tau^{12}$ (equations 5.14 and 5.15), which treat the effect of the host lattice sites realistically, are considered for computation and for physical reasons $\tau^{11}$ and $\tau^{12}$ are equal to $\tau^{22}$ and $\tau^{21}$ respectively (also numerically tested). The matrices $\tau^{11}$ and $\tau^{12}$ involve Brillouin zone integrations via equations (5.14) and (5.15). These fairly complicated Brillouin zone (B.Z.) integrations for fcc crystals are evaluated using the special directional methods (Stocks et al 1979) within the KKR band theory framework. The special directions in 1/48-th of the irreducible B.Z. for fcc crystal can be calculated either by the Prism method (Stocks et al 1979) or by Bansil's special direction method (Bansil 1975). The special directions are projected on the 48 irreducible zones using the 48 symmetry operations of the cubic group for cubic structures and hence the integration over

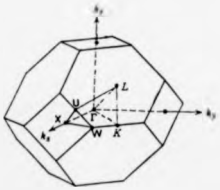


Figure 6.1: Brillouin zone for an fcc crystal and the irreducible 1/48-th zone.

the whole B.Z. is done. In section (6.2), the computational procedure for $\tau^{ij}$ $(i,j = 1,1$ or $1,2)$ is presented. In section (6.3), the energy integration for equation (5.24) is described in terms of the Matsubara sum (Fetter and Walecka 1972). In section (6.5), all the results for the two Fe impurities in both Au and Cu host are presented for different orientations of the impurity spins. A discussion on the results is presented in section (6.5)

## 6.2 Computational procedure of $\tau^{ij}$ $(i,j = 1,1$ or $1,2)$

In this section, the computational technique for $\tau^{ij}$ $(i,j = 1,1$ or $1,2)$ is discussed. Recalling equations (5.14) and (5.15), the matrix $\tau^{ij}$ in the l, m and $\sigma$ representation is

$$\tau^{ij}_{lm\sigma,l'm'\sigma'}(E) = \frac{1}{\Omega_{B.Z.}} \int_{B.Z.} d\underline{k} [(t^{\sigma^{-1}} - G^{\sigma}(\underline{k},E))^{-1}]_{lm\sigma,l'm'\sigma'} e^{i\underline{k}.\underline{R}_{ij}} \qquad (6.1)$$

where $\underline{R}_{ij}$ is the separation vector between two impurities on sites $i$ and $j$. Suppressing all the subscript and the superscripts, for convenience,

$$\tau(\underline{k},E) = (t^{\sigma^{-1}} - G^{\sigma}(\underline{k},E))^{-1} \qquad (6.2)$$

Therefore,

$$\tau^{ij}(E) = \frac{1}{\Omega_{B.Z.}} \int_{B.Z.} d\underline{k} \;\; \tau(\underline{k},E) e^{i\underline{k}.\underline{R}_{ij}} \qquad (6.3)$$

where $\tau(\underline{k},E)$ is the function to be integrated over the Brillouin zone. For this purpose, the volume integration has to be transformed into a sum of weighted line integrals. Following

Stocks et al (1978), the line integral $\tau^{\hat{k}_l}$ of the function of interest, $\tau(\underline{k}, E)$, along the $l$-th direction can be defined

$$\tau^{\hat{k}_l}(E) = \frac{1}{\Omega_{B.Z.}} \int_0^{k_l^{B.Z.}} dk_l \omega(k_l) \tau(\underline{k}_l, E) \tag{6.4}$$

where $\omega(k_l)$ is appropriate radial function and $k_l^{B.Z.}$ denotes the Brillouin zone boundary along the direction $\hat{k}_l$. The required integral (6.3) can be approximated by summing over the line integrals for $N-$directions, choosing $\omega(k_l) = k_l^2$,

$$\tau^{ij}_{lm\sigma,l'm'\sigma'} = \frac{1}{\Omega_{B.Z.}} \sum_{l=1}^{N} \omega_l [\sum_{n=1}^{48} \int_0^{k_{l_1}^{B.Z.}} dk_{l_1}^n . k_{l_1}^{n^2} . \tau_{lm\sigma,l'm'\sigma'}(k_{l_1}^n, E) e^{i\underline{k}_{l_1}^n . \underline{R}_{ij}}] \tag{6.5}$$

where $\omega_l$ is some appropriate weight function, "1" refers to the first irreducible part, $l$ is for the special lines. According to equation (6.5), the integrand is first calculated along one special direction in the one irreducible 1/48-th of the Brillouin zone, then, the summation is taken over the 48 segments using the symmetry operations of the cubic group and special directional wave vectors cover the whole B.Z. Thus the integration is evaluated for one special direction $k_l$ at a time. Finally, the summation over all the special lines gives the total volume integration done. For calculating $\tau^{12}$, $\underline{R}_{12}$ is a fixed value and the exponential phase factor $e^{i\underline{k}.\underline{R}_{12}}$ is included in the integration. For calculating $\tau^{11}$, $\underline{R}_{12}$ is equal to zero and the exponential factor is set equal to unity.

In this calculation Bansil's (Bansil 1975) 13 special directions are used. Bansil (1975) calculated the intersection of the special direction emanating from the B.Z. center through the (100) face of the reciprocal lattice for $\omega_l$=1. In table 1, the intersections for 5 and 13 special directions with the surface of the 1/48-th B.Z. are presented along with the Bansil's (1975) special directions. The convergency of this integration is checked using the relation (Callaway 1974)

$$\frac{1}{\Omega_{B.Z.}} \int_{B.Z.} \underline{dk} e^{i\underline{k}.(\underline{R}_1 - \underline{R}_2)} = \delta_{12} \tag{6.6}$$

For two well separated impurity sites, the l.h.s. of this equation for both 5 and 13 lines with 10, 30, 50, 100 points is computed and it begins to vanish for 13 lines as the number

Table 6.1: Special lines in the 1/48-th irreducible BZ.

| Intersection of the special directions passing through (100) face of the reciprocal lattice (Bansil 1975) | Intersection of the special direction passing through the surface of the irreducible BZ. | Corresponding $l_{max}$ (Maximum order of the cubic harmonic). |
|---|---|---|
| (1.0, 0.83947, 0.20191) | (0.7348, 0.61684, 0.14836) | |
| (1.0, 0.22094, 0.07718) | (1.0, 0.22094, 0.07718) | |
| (1.0, 0.86383, 0.60255) | (0.608179, 0.52536, 0.366458) | 18 |
| (1.0, 0.54291, 0.10739) | (0.90893, 0.49347, 0.09761) | |
| (1.0, 0.44845, 0.37186) | (0.824035, 0.36954, 0.306426) | |
| (1.0, 0.13103, 0.10582) | (1.0, 0.13103, 0.10582) | |
| (1.0, 0.24802, 0.10523) | (1.0, 0.24802, 0.10523) | |
| (1.0, 0.35398, 0.07736) | (1.0, 0.35398, 0.07736) | |
| (1.0, 0.40889, 0.29697) | (0.879319, 0.35955, 0.261133) | |
| (1.0, 0.61649, 0.05975) | (0.89486, 0.55167, 0.053468) | |
| (1.0, 0.63223, 0.29730) | (0.77739, 0.49149, 0.23112) | |
| (1.0, 0.54055, 0.38147) | (0.78043, 0.421861, 0.29771) | 20 |
| (1.0, 0.72186, 0.5238) | (0.66796, 0.48217, 0.349874) | |
| (1.0, 0.86139, 0.74881) | (0.574668, 0.495014, 0.4303176) | |
| (1.0, 0.86312, 0.43258) | (653395, 0.563959, 0.282646) | |
| (1.0, 0.87096, 0.02398) | (0.791582, 0.68944,0.018982) | |
| (1.0, 0.46248, 0.17268) | (0.9173414, 0.424252, 0.1584065) | |
| (1.0,0.79460, 0.24975) | (0.73373, 0.5830215, 0.18324895) | |

of points increases from 30. Accuracy in the numerical integration can be achieved by adding more and more points on the lines. In the next section, the numerical technique for the energy integration (5.24) is presented and $\tau^{11}$, $\tau^{12}$, $\tau^{22}$ and $\tau^{21}$ are calculated at complex energies to use in this expression.

## 6.3 The calculational method of the expression (5.24)

In evaluating the integration in expression (5.24) it is expressed as a sum over Matsubara frequencies (Fetter and Walecka 1972) to avoid the poles on the real energy axis contained in $\tau^{11}, \tau^{22}, \tau^{12}$ and $\tau^{21}$. Recalling expression (5.24), the interaction energy between two Fe magnetic impurities in both the Au and Cu hosts is

$$E_{12} = (-2k_BT)\sum_{n=0}^{\infty}\sum_{\Lambda_1\Lambda_2\Lambda_3\Lambda_4\Lambda_5} M^2_{\Lambda\Lambda_1}(\nu+i\omega_n)\tau^{12}_{\Lambda_1\Lambda_2}(\nu+i\omega_n)\Delta_{2,\Lambda_2\Lambda_3}(\nu+i\omega_n) \times M^2_{\Lambda_3\Lambda_4}\tau^{21}_{\Lambda_4\Lambda_5}(\nu+i\omega_n)\Delta_{1,\Lambda_5\Lambda}(\nu+i\omega_n) \quad (6.7)$$

where $k_B = 0.63333 \times 10^{-5}$ Ryd./$^oK$ is the Boltzman constant, $\nu$ is the chemical potential appropriate to a system and the Matsubara frequency $\omega_n = (2n+1)\pi k_BT$, where $n = 0, 1, 2, \ldots$ integers. Owing to the presence of complex energies in the above Matsubara sum, the t-matrix is calculated at complex energies following the method discussed in chapter 2. The Matsubara sum is evaluated on a logarithmic mesh for 25 values of the imaginary energy part $\omega$ from 0.005 to 1.256 Rydberg instead of the direct sum over many Matsubara frequencies and the results are interpolated to the required Matsubara frequencies. As the imaginary energy part increases, the contribution to the interaction energy between the two impurities decreases and hence the sum can be cutoff at $\simeq$ 1.0 Ryd.(1.256 is used).

## 6.4 The effective exchange parameter

The effective exchange parameter, $J_{ij}$, for two impurity spins at $i$ and $j$ can be defined (Oguchi et al 1983) as

$$J_{ij} = -(E^F_{ij} - E^{AF}_{ij})/2S^2 \quad (6.8)$$

where $E_{ij}^{P}$ is the interaction energy for two parallel spins and $E_{ij}^{AP}$ is the interaction energy for two antiparallel spins. $S$ is the magnitude of the impurity atomic spins. All the calculations are done for a fixed temperature $T = 300^{o}K$ in the Matsubara sum. In the next section, all the results are presented.

## 6.5 RESULTS

### 6.5.1 Euler angles made by the two impurity spins.

In Table6.2the appropriate angles to specify the various arrangements of the two impurity spins with respect to the crystal axes are presented — the first set describes the two impurity spins parallel to each other and perpendicular to the separation vector $R_{12}$; the second set describes the two spins parallel both to each other and the separation vector $R_{12}$, and thirdly the two spins antiparallel to each other and perpendicular to the separation vector $R_{12}$. Throughout the calculation the Euler angles $\alpha$ are kept constant and fixed at zero and the equations (5.21) and (5.22) are used. The Euler angles convert the $t$-matrix calculated in the "local" frame (with the magnetic component of the impurity potential oriented along the local Z-axis), $t^{local}$, into the $t$-matrix in the working frame, $t^{working}$, through the relation (2.45). In this thesis, the inverse of $t^{local}$ is transformed into the inverse of $t^{working}$ via the relation (5.17) using the Euler angles.

### 6.5.2 The anisotropic interaction energy, its anisotropic components and the effective exchange parameter between two Fe impurities in Au host.

In table 6.3, using table 6.2, the relativistic interaction between two iron impurity spins $S_1$ and $S_2$ in a cubic fcc Au host, its anisotropic components ($E_{12}^{\uparrow\uparrow} - E_{12}^{\uparrow\downarrow}$) and effective exchange parameter are calculated for various separations $R_{12}$, while the spin $S_1$ is fixed at the origin. The anisotropic components calculated by Staunton et al (1988) for the corresponding separations are also presented in the same table for a clear comparison.

Table 6.2: Euler angles made by the two impurity spins $\hat{S}_1$ and $\hat{S}_2$ for various positions of the second spin $S_2$ in an fcc crystal structure. The first spin $S_1$ is fixed at the origin. The Euler angles $\alpha_1$ and $\alpha_2$ made by $S_1$ and $\bar{S}_2$ respectively are set equal to zero.

| Separation vector $\bar{R}_{12}$ in (a.u) | Diagram for two impurities in fcc crystal (with n=1) | Euler angles for $\hat{S}_1$ and $\hat{S}_2 \perp$ to $\bar{R}_{12}$ (in deg.) $\gamma_1 = \gamma_2$ $\beta_1 = \beta_2$ | | Euler angles for $S_1$ and $\hat{S}_2 \parallel$ to $\bar{R}_{12}$ (In deg.) $\gamma_1 = \gamma_2$ $\beta_1 = \beta_2$ | | Euler angles for $\bar{S}_1$ and $\hat{S}_2 \perp$ to $\bar{R}_{12}$, but $\hat{S}_1 = -\bar{S}_2$ $\gamma_1$ $\beta_1$ $\gamma_2$ $\beta_2$ | | | |
|---|---|---|---|---|---|---|---|---|---|
| $(n\pi, n\pi, 0)$ |  | 0 | 0 | 45 | 90 | 0 | 0 | 0 | 180 |
| $(0, n2\pi, 0)$ |  | 0 | 0 | 90 | 90 | 0 | 0 | 0 | 180 |
| $(n\pi, n2\pi, n\pi)$ |  | -63.44 | 24.09 | 63.44 | 65.91 | -63.44 | 24.09 | 63.44 | 155.91 |
| $(n\pi, n3\pi, 0)$ |  | 0 | 0 | 18.43 | 90 | 0 | 0 | 0 | 180 |
| $(n2\pi, n2\pi, n2\pi)$ | 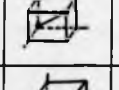 | -45 | 35.26 | 45 | 54.75 | -45 | 35.26 | 45 | 144.74 |
| $(n3\pi, n2\pi, \pi)$ |  | -33.69 | 15.50 | 33.69 | 74.50 | -33.69 | 15.50 | 33.69 | 164.50 |

Table 6.3: Relativistic interaction between two Fe impurities, anisotropic interaction and the effective exchange parameter in an fcc Au host. These refer to configurations shown in table (6.2) and are in Rydbergs.

| Position of the second spin $S_2$ in (a.u) $\vec{R}_{12}$ | Interaction energy for both impurity spins $\perp$ to $\vec{R}_{12}$ $E_{12}^{\uparrow\uparrow}$ ($\times 10^{-03}$) | Anisotropic interaction energy ($E_{12}^{\uparrow\uparrow} - E_{12}^{\uparrow\downarrow}$) ($\times 10^{-04}$) | Anisotropic interaction energy by Staunton et al (1988) ($\times 10^{-06}$) | Effective exchange parame $J_n$ ($\times 10^{-03}$) |
|---|---|---|---|---|
| $(\pi, \pi, 0)$ | -34.570 | +4.190 | | +5.8970 |
| $(0, 2\pi, 0)$ | -51.700 | -5.010 | | -0.7414 |
| $(\pi, 2\pi, \pi)$ | -4.490 | +2.135 | -4.5 | +0.8809 |
| $(2\pi, 2\pi, 0)$ | -13.700 | -2.875 | +3.5 | +1.3760 |
| $(\pi, 3\pi, 0)$ | -0.380 | +0.803 | +4.6 | +0.2634 |
| $(2\pi, 2\pi, 2\pi)$ | -4.690 | 0.740 | -0.40 | +0.0986 |
| $(3\pi, 2\pi, \pi)$ | -0.123 | +1.541 | -3.5 | +0.0119 |
| $(0, 4\pi, 0)$ | -0.989 | +3.110 | -2.0 | +0.3776 |
| $(3\pi, 3\pi, 0)$ | -0.900 | -1.208 | +1.2 | +0.2589 |
| $(2\pi, 4\pi, 0)$ | +0.652 | +0.335 | +2.6 | -0.258 |
| $(4\pi, 4\pi, 0)$ | -1.230 | -1.139 | | |
| $(0, 6\pi, 0)$ | +0.098 | +3.254 | | |
| $(5\pi, 5\pi, 0)$ | -2.250 | +0.0525 | | |
| $(6\pi, 6\pi, 0)$ | -1.430 | +0.130 | | |
| $(0, 8\pi, 0)$ | +0.041 | +0.052 | | |

Although the order of the interaction between two Fe impurities in the Au host calculated in this thesis is the same as that calculated for the jellium model by Staunton et al (1988), the anisotropic effect is remarkably enhanced. The effective exchange parameters are of the same order as the corresponding two site interactions. In fig.(6.2), the relativistic interaction between the two Fe impurities versus the separation $R_{12}$ are plotted for two directions [010] and [110]. Qualitatively these curves are neither of the usual RKKY form nor of the relativistic RKKY form. The curve for along [010] direction is critically damped, while for along [110] it is of damped oscillatory type and pulled down. In fig.6.3, the anisotropic component versus separation curves are also plotted for the same two directions and the anisotropic effect, which is found to be enhanced, in the two site interaction is oscillatory. The Fe potential constructed self-consistently by Moruzzi et al (1978) is used through out the calculations.

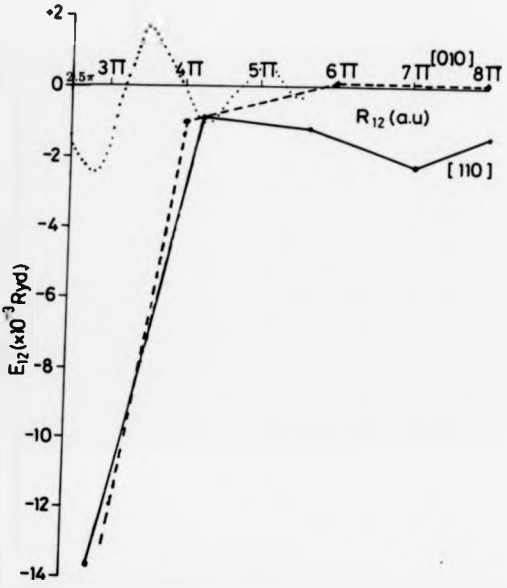


Figure 6.2: Relativistic interaction between two Fe impurities in a Au host as a function of separation. The solid line shows the interaction between two Fe spins which are both perpendicular to $R_{12}$ along the [110] direction, while the broken line is for $R_{12}$ along [010]. The dotted line is for the relativistic RKKY interaction calculated by Staunton et al (1988)

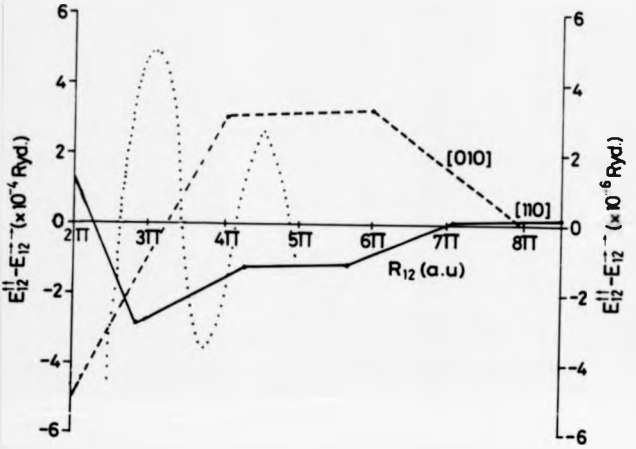


Figure 6.3: The anisotropic component ($E_{12}^{11} - E_{12}^{\bar{1}\bar{1}}$) versus separation curves for two Fe impurities in Au host. The solid line is drawn for the anisotropic component along the [110] direction, while the broken line is for along the [010] direction (left vertical axis). The dotted curve shows the anisotropic component versus separation calculated by Staunton et al (1988) (right vertical axis).

### 6.5.3 The anisotropic effect with respect to both separation vector and the crystal axes.

In fig.6.4, constructed from table 6.4(a), first a solid line is plotted with spin 1 fixed along the crystallographic Z-axis, while the spin 2 takes range of angles from $+90^o$ to $-90^o$ with separation $R_{12}(0, 4\pi, 0)$, rotating in the $YZ-$plane. The anisotropy field is minimum for the case of the lower end of this curve. The dotted curve is plotted, using table6.4b , for spins 1 and 2 parallel to each other and rotating in the $YZ$-plane making a range of angles from $90^o$ to $-90^o$ with respect to $R_{12}(0, 4\pi, 0)$. The two extreme points of the dotted curve preserves the mirror reflection symmetry of the interaction through a vertical plane and the anisotropy field is largest when both $\hat{S}_1$ and $\hat{S}_2$ are parallel to $R_{12}(0, 4\pi, 0)$.

In fig.6.5, using table 6.4(c), the solid line, which is varying sinusoidally, is plotted for parallel spins 1 and 2 rotating in the $XY$-plane making angles from $0^o$ to $180^o$ with respect to $R_{12}(0, 4\pi, 0)$. The interaction energies for the cases of the two extreme points are equal and largest. In the same figure, using table6.4d , the broken line is plotted for both 1 and 2 parallel and rotating in the $XZ$-plane making angles $0^o$ to $180^o$ with the crystal axis, while both $\hat{S}_1$ and $\hat{S}_2$ make an angle of $90^o$ with $R_{12}(0, 4\pi, 0)$. The broken line shows a very weak growing anisotropy with respect to the crystal axis, however, the solid curve shows a strong growing anisotropy with respect to the separation vector $R_{12}$. Thus the spin-orbit interaction couples the spins very weakly to the crystal axes as well as a stronger coupling to the separation vector $R_{12}$.

### 6.5.4 The "exchange degeneracy" of the interaction and symmetry properties of both the relativistic two site interaction and its anisotropic effect.

From table 6.5(a), it appears that the interaction between two impurity spins is invariant under the exchange of the two spins and the anisotropy contained in this two site interaction is termed as a uniaxial anisotropy (Chikazumi 1964, Staunton et al 1989). On swapping the two spins the same environment in the fcc cubic host is found on symmetry

Table 6.4(a) Relativistic interaction between two Fe impurities described by spin $\hat{S}_1$ which is aligned with a crystal axis and by spin $\hat{S}_2$ which takes a range of angles from $+90°$ to $-90°$ rotating within the $YZ$-plane. $\boldsymbol{R}_{12} = (0, 4\pi, 0)$.

| Spin arrangements on $YZ$-plane with $\boldsymbol{R}_{12} = (0, 4\pi, 0)$ | $\boldsymbol{R}_{12} \cdot S_2$ in degrees. | Interaction energy $E_{12}$ in Ryd. ($\times 10^{-03}$) |
|---|---|---|
| 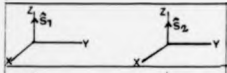 | 90 | -0.988604 |
| 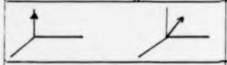 | 60 | -0.962059 |
| 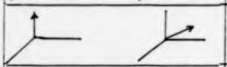 | 30 | -0.890771 |
| 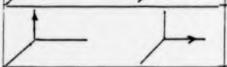 | 0 | -0.764114 |
| 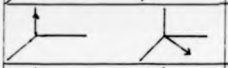 | -30 | -0.554686 |
| 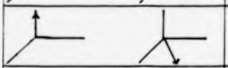 | -60 | -0.330181 |
| 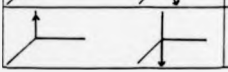 | -90 | -0.23319 |

Table 6.4(b) Relativistic interaction between two Fe impurities with spins rotating in the $YZ$-plane such that $\hat{S}_1$ and $\hat{S}_2$ are parallel to each other and make a range of angles from $+90°$ to $-90°$ with $\vec{R}_{12} = (0, 4\pi, 0)$.

| Spin arrangements on $YZ$-plane with $\vec{R}_{12} = (0, 4\pi, 0)$ | $\vec{R}_{12}.\hat{S}_1$ and $\vec{R}_{12}.\hat{S}_2$ in deg. | Interaction energy $E_{12}$ in Ryd. ($\times 10^{-03}$) |
|---|---|---|
|  | 90 | −0.988604 |
|  | 60 | -1.055232 |
|  | 30 | -1.210551 |
| 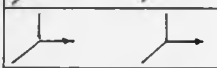 | 0 | -1.299605 |
| 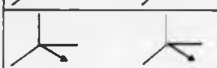 | -30 | -1.210552 |
|  | -60 | -1.055232 |
| 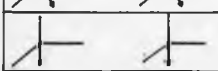 | 90 | −0.988604 |

Table 6.4(c) Relativistic interaction between two Fe impurities described by spins rotating in the $XY$-plane such that $\vec{S}_1$ and $\vec{S}_2$ are parallel to each other and make a range of angles from $0^o$ to $180^o$ with $\vec{R}_{12} = (0, 4\pi, 0)$.

| Spin orientations on $XY$-planes. | $\vec{R}_{12}.\vec{S}_1$ and $\vec{R}_{12}.\vec{S}_2$ (in degree). | Interaction $E_{12}$ in Rydberg ($\times 10^{-03}$) |
|---|---|---|
| 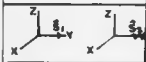 | 0 | -1.299605 |
|  | 30 | -1.21055 |
|  | 45 | -1.129126 |
| 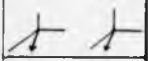 | 60 | -1.055226 |
|  | 90 | -0.9885946 |
| 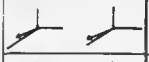 | 120 | -1.055226 |
| 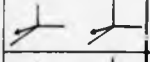 | 135 | -1.129126 |
| 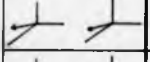 | 150 | -1.21055 |
| 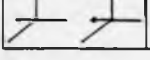 | 180 | -1.299605 |

Table 6.4(d) Relativistic interaction between two Fe impurities described by spins rotating in the $XZ$-plane such that $\vec{S}_1$ and $\vec{S}_2$ are parallel to each other and make a range of angles from 0° to 180° with the crystal axis and $\vec{R}_{12} = (0, 4\pi, 0)$.

| Spin orientations on on $XZ$-planes. | Angles made by $\vec{S}_1$ and $\vec{S}_2$ with crystal axis (in deg.). | Interaction energy $E_{12}$ in Rydberg ($\times 10^{-03}$) |
|---|---|---|
| 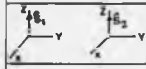 | 0 | -0.988604 |
| 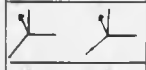 | 30 | -1.02001 |
| 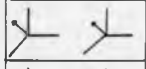 | 45 | -1.030514 |
| 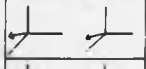 | 60 | -1.020005 |
| 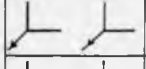 | 90 | -0.9885946 |
| 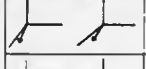 | 120 | -1.020005 |
| 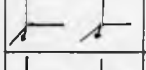 | 135 | -1.030514 |
| 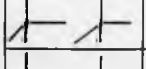 | 150 | -1.02001 |
| 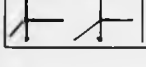 | 180 | -0.988604 |

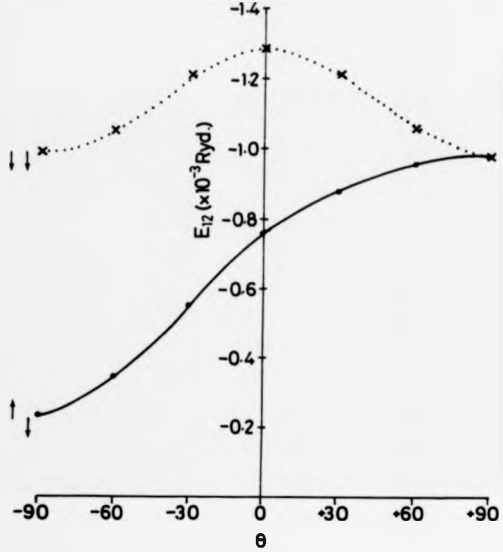


**Figure 6.4:** Relativistic interaction versus angle of rotation of the impurity spins. (a) The solid line shows the case for spin 1 aligned with the crystal $Z$-axis and spin 2 rotating within $YZ$-plane. (b) The dotted line is for both spin 1 and 2 rotating within the $YZ$-plane.

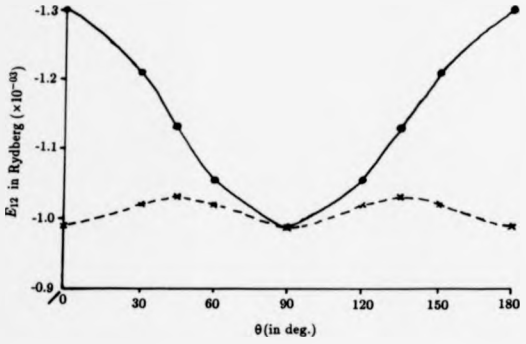


Figure 6.5: Relativistic interaction versus angle of rotation of the impurity spin. (a) The solid line is drawn for spins 1 and 2 rotating simultaneously in the $XY$-plane making an angle with $R_{12} = (0, 4\pi, 0)$. (b) The broken line is drawn for spins 1 and 2 rotating simultaneously in the $ZX$-plane making an angle with the crystal axis.

Table 6.5(a) Relativistic "exchange" interaction between two Fe impurity spins with separation vector $R_{12} = (0, 4\pi, 0)$.

| Spin arrangements in $XY$-plane. | Interaction energy $E_{12}$ in Ryd.($\times 10^{-03}$). |
|---|---|
| 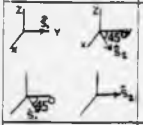 | -1.125209 |
| | -1.125209 |
|  | -0.541157 |
| | -0.541157 |

grounds and the inversion symmetry for the interaction with respect to the mid-point is preserved in this circumstance. In table 6.5(b), the relativistic interactions and the anisotropic components for six configurations with the second impurity spin on the 8-th neighbouring shell are presented and found to be the same. This symmetry can reduce the theoretical calculation to study such magnetic properties of dilute alloys. To interpret these results, interactions between two Fe impurities are calculated by treating Fe impurity sites relativistically and host sites non-relativistically and vice versa. The results are presented in the following sub-section.

### 6.5.5 Results for Fe sites treated relativistically and Au sites treated non-relativistically and vice versa.

In table 6.6(a), the interaction between the two Fe impurities and its anisotropic components are presented for Fe scattering sites treated relativistically and the Au host sites treated non-relativistically for separations up to seven nearest neighbours. In this case, the two site interaction and the anisotropic interaction are of the same order of those calculated in the relativistic jellium model (Staunton et al 1988). In table 6.6(b), Fe sites are

Table 6.5(b) Relativistic interaction and the anisotropic interaction to check the symmetry.

| Position of the 2nd Fe impurity spin $R_{12}$. | Interaction energy $E_{12}^{11}$ in Ryd. ($\times 10^{-03}$) | Anisotropic interaction energy $(E_{12}^{11} - E_{12}^{\rightarrow\rightarrow})(\times 10^{-06})$. |
|---|---|---|
| $(0, 4\pi, 0)$ | -0.9886 | 3.110 |
| $(4\pi, 0, 0)$ | -0.9886 | 3.110 |
| $(0, 0, 4\pi)$ | -0.9886 | 3.110 |
| $(-4\pi, 0, 0)$ | -0.9886 | 3.110 |
| $(0, 0, -4\pi)$ | -0.9886 | 3.110 |
| $(0, -4\pi, 0)$ | -0.9886 | 3.110 |

treated non-relativistically and the Au host sites are treated relativistically. These results are very close to the results found for the relativistic two site Fe impurities presented in table6.3and this suggests the importance of the relativistic treatment of the host sites. In the next sub-section, relativistic interaction between two Fe impurities in a Cu host is studied to see the effect of a light paramagnetic host on the anisotropic component in relativistic two site interaction.

### 6.5.6 Results for the relativistic interaction between two Fe impurities in a Cu host.

In table 6.7, the relativistic interaction between two Fe impurities in a Cu host and its anisotropic components are also presented for up to the seven nearest neighbours. In this case, although copper (Z=29) is host of low atomic number, the anisotropic components are still enhanced though smaller than that for AuFe by an order of magnitude. In this calculation, the two site interaction is changing sign with separation more rapidly than the relativistic two site interaction for AuFe and thus the two site interaction can be closer to the relativistic RKKY interaction for a host of very low atomic number.

Table 6.6(a) Interaction between two Fe impurities where the Fe sites are treated relativistically and the gold host sites are treated non-relativistically.

| Position of the 2nd neighbouring atom (in a.u.). | Interaction between two Fe spins in Ryd. $E_{12}^{\uparrow\uparrow}$ ($\times 10^{-03}$) | Anisotropic interaction energy $E_{12}^{\uparrow\uparrow} - E_{12}^{\uparrow\downarrow}$ (in $\times 10^{-06}$ Ryd.) | Anisotropic interaction energy by Staunton et al (1988) (in $\times 10^{-06}$ Ryd.) |
|---|---|---|---|
| (0,2$\pi$,0) | -4.59917 | +3.516 | |
| ($\pi$, 2$\pi$, $\pi$) | -2.59686 | +0.1220 | -4.3 |
| (2$\pi$, 2$\pi$, 0) | -1.129404 | -1.1960 | +2.8 |
| ($\pi$, 3$\pi$, 0) | -0.481211 | -0.2180 | +4.9 |
| (0, 4$\pi$, 0) | +0.819559 | +1.2090 | -2.0 |
| (2$\pi$, 2$\pi$, 2$\pi$) | -1.25048 | -0.0430 | -0.40 |
| (3$\pi$, 2$\pi$, $\pi$) | -0.0136811 | +0.2390 | -3.5 |

Table 6.6(b) Interaction between two Fe impurities where the Fe sites are treated non-relativistically and the gold host sites are treated relativistically.

| Position of the 2nd neighbouring atom (in a.u.). | Interaction between two Fe spins in Ryd. $E_{12}^{\uparrow\uparrow}$ ($\times 10^{-03}$) | Anisotropic interaction energy $E_{12}^{\uparrow\uparrow} - E_{12}^{\uparrow\downarrow}$ (in $\times 10^{-04}$ Ryd.) |
|---|---|---|
| (0,2$\pi$,0) | -57.61646 | -2.6084 |
| ($\pi$, 2$\pi$, $\pi$) | -4.909871 | +2.31039 |
| (2$\pi$, 2$\pi$, 0) | -14.53908 | -3.7620 |
| ($\pi$, 3$\pi$, 0) | -0.351744 | +1.8581 |
| (0, 4$\pi$, 0) | -1.010089 | +4.54874 |
| (2$\pi$, 2$\pi$, 2$\pi$) | -5.357655 | +0.94729 |
| (3$\pi$, 2$\pi$, $\pi$) | -0.1132078 | +1.6946 |

Table 6.7 Relativistic interaction between two Fe impurities in Cu host and the anisotropic component.

| Position of the 2nd neighbouring atom (in a.u.). | Interaction between two Fe spins in Ryd. $E_{12}^{\uparrow\uparrow}$ ($\times 10^{-03}$) | Anisotropic interaction energy $E_{12}^{\uparrow\uparrow} - E_{12}^{\uparrow\downarrow}$ (in $\times 10^{-06}$ Ryd.) |
|---|---|---|
| (0,2π,0) | -20.6495 | +5.5460 |
| (π, 2π, π) | +1.32473 | -0.4955 |
| (2π, 2π, 0) | -3.208756 | -1.0116 |
| (π, 3π, 0) | +0.257756 | -1.0606 |
| (0, 4π, 0) | +0.128633 | -0.3512 |
| (2π, 2π, 2π) | +0.023879 | +0.0911 |
| (3π, 2π, π) | -0.1253297 | +0.2659 |

## 6.6 DISCUSSION

The relativistic expression (5.24) for the interaction between two magnetic impurities in a realistic paramagnetic host contains an anisotropic effect. As the expression contains a dependence upon the band structure of the host, and is therefore a realistic approach to cope with the individual lattice sites of the host, it is in effect a multi-atom interaction, describing the interaction between the two magnetic impurities and all the multiple scattering effects of the host in between. This expression can be trivially reduced to that of Staunton et al's (1988) "the relativistic RKKY interaction between two magnetic impurities" in a jellium model background as shown in the appendix (A). The reduced expression contains the anisotropic effect through its polynomial dependence upon a squared Dzyaloshinsky-Moriya term and a pseudo-dipolar term as in eq.(4.14) (Staunton et al 1988). Although from the key expression (5.24) of this thesis the anisotropic effect is not obvious at once, it is demonstrated through the numerical computation. The Dzyaloshinsky-Moriya term, which appeared in Fert et al's(1980) anisotropic two site interaction, breaks the inversion symmetry of the two site interaction with respect to the mid-point between the two im-

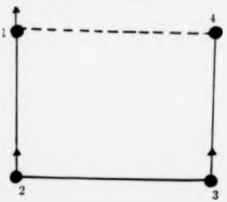


Figure 6.6: The solid line is for ferromagnetic exchange interaction energy and the broken line is for the antiferromagnetic exchange interaction energy. Spin 4 is "frustrated" in this diagram.

purity spins and this anisotropic interaction is regarded as the unidirectional anisotropy. As mentioned earlier in section (6.5.4), the anisotropic interaction found in this thesis is termed as a uniaxial anisotropy, because the inversion symmetry for the interaction with respect to the mid-point is preserved in this circumstance (cf. table 6. 5(a)). The mathematical origin of this two site anisotropic interaction may be more complicated than the relativistic RKKY interaction found by Staunton et al (1988).

In fig 6.2, the relativistic interaction between the two Fe impurities in a Au host is a critically damped oscillation function of the separation $R_{12}$ along the [010] direction, while along the [110] direction this is of damped oscillatory type and pulled down. Although, these curves are not of the usual oscillatory RKKY form, a "frustration effect" is still added to the spin glass system. The concept of "frustration", for which some impurity spin is not satisfied with the two site interaction due to its sign change, (because for positive interaction energy between two impurity spins, they are thought to be aligned parallel while for negative energy they are aligned anti-parallel) is important in studying the ground state configuration of spin glasses (Toulouse 1977). The anisotropic components $(E_{12}^{\uparrow\uparrow} - E_{12}^{\uparrow\downarrow})$ which are $\sim 10^{-04}$ Rydberg and comparable to the interaction itself, are found to be enhanced by two orders of magnitude for two substitutional Fe impurities in a Au host over that for the anisotropic components calculated by Staunton et al (1988)

for two Fe impurities in a relativistic jellium model, which is $\sim 10^{-08}$ Rydberg. Although both Fert et al (1980) and Staunton et al (1988) predicted an enhanced two site anisotropic effect by incorporating a realistic host, they did not estimate the size of the effect. So, for studying a dilute magnetic alloy the relativistic spin-orbit interaction, which is the principal source of the anisotropic effect cannot be justified as a small perturbation. This work is the first attempt at determining the size of this effect.

The anisotropic components shown in fig.6.3 as a function of separation along both [110] and [010] directions are also found to be oscillatory in nature and subsequently add another kind of "anisotropic frustration" to the spin glass system. This enhanced anisotropic effect along with the "frustration effect" can be important in the study of the qualitative nature of a spin glass and a better understanding of dilute magnetic alloys can be achieved.

In fig.6.4 and fig.6.5, the growing anisotropy is studied by rotating the impurity spins with respect to both $\hat{R}_{12}$ and the crystal axes. In fig.6.4, the interaction energy exhibits a peak for both spins aligned parallel to $\hat{R}_{12}$ and this can be the result of the pseudo-dipolar type term, $(\hat{R}_{12}\cdot\hat{S}_1)(\hat{R}_{12}\cdot\hat{S}_2)$, because for spins both parallel to each other and parallel to $\hat{R}_{12}$ the term is largest and for this spin arrangement the D.M term $(\hat{R}_{12}\cdot(\hat{S}_1 \times \hat{S}_2))$ is zero. However, this two site uniaxial anisotropic interaction is not simply dependent on either the pseudo-dipolar term or the D.M. term or both. The anisotropic effect in this interaction may be contained through some additional terms, which may be complicated and difficult to extract analytically. A unidirectional anisotropy can be contained in this two site interaction either by considering the potentials of two impurities to be a little different or considering a third impurity site in this calculation. The inversion symmetry about the midpoint of the two sites is broken in this way.

In table 6.6(a), the interaction between two relativistically treated Fe impurities is calculated in a Au host treated non-relativistically and the interaction and its anisotropic components are found nearly in the same order as for the two Fe impurities in a jellium model (Staunton et al 1988). This suggests that the non-relativistic treatment of the

host lattice medium produces no qualitative differences to the anisotropy effects inferred from the uniform positively charged background (or relativistic jellium) model. On the other hand the interaction and the anisotropic component for the two non-relativistic Fe impurities in a relativistically treated Au host in table 6.6(b) is almost of the same order as the relativistic interaction and its anisotropic component. This also suggests that the relativistic treatment of a heavy paramagnetic host has the greater influence on the anisotropic effect. The relativistic interaction and the anisotropic effect for two Fe impurities in Cu host of low atomic number (Z=29) are also studied. From the results in table 6.7, the anisotropic components, which are $\sim 10^{-05}$ Rydberg, are found to be also enhanced by the relativistic treatment of a host of low atomic number in this case. So, to study a dilute magnetic alloy system, the relativistic treatment of the host realistically is crucial and this new relativistic interaction between the magnetic impurities can serve well for studying the properties of a dilute magnetic alloys. In the next chapter, a conclusion of this thesis is presented.

# Chapter 7

# CONCLUSION

The main objective of this thesis has been to study the relativistic interaction between two magnetic impurities and the origin of magnetic anisotropic effect for a problem of dilute magnetic alloys incorporating the crystalline nature of the host realistically. The entire formalism of the theory and its computational technique to study the two site interaction and the anisotropic effect has been based on relativistic spin polarised multiple scattering theory and the related relativistic (KKR) band structure calculation. The idea of the "working" frame of reference, which was set up in section 5.3 with its axes oriented along the fcc crystal axes, has been used so that the orientations of the magnetic moments on the impurity sites in the environment of this host crystal could be varied. This was achieved by rotating the $t$-matrix (which is calculated using spin-polarised scattering theory for a potential on the impurity site with its magnetic component oriented along local $Z$-axis). In this way the magnetic anisotropic effect of these systems was studied.

The theory for the relativistic two site interaction has been derived by considering the two magnetic impurity sites far apart and thus it is applicable to the case of dilute magnetic alloys. This simplification can be relaxed and the magnetic properties of higher concentration transition metal-noble metal alloys and the magnetic anisotropic effects of two spatially close magnetic impurities can be studied by retaining the logarithm in equation (5.10). The anisotropic effect in expression (5.24), which is deduced for the

relativistic interaction between two magnetic impurities in a realistic host, has no clear analytic form and it has therefore been studied through computation.

The results of this thesis, which has been presented in section 6.5 can be summarised, firstly, recalling that the relativistic interaction between two Fe impurities in a realistic Au host has been found to be a critically damped oscillatory function of separation along [010] and of damped oscillatory type along [110]. These results have ruled out the possibility of existence of a simple sinusoidal oscillating RKKY and R-RKKY (Staunton et al 1988) interaction between two magnetic impurities in a heavy paramagnetic host. In table 6.7, the relativistic interaction has been shown to change sign for two Fe impurities in Cu host as the separation is varied more rapidly than in AuFe. Thus, still the RKKY or the R-RKKY interaction can exist in shape for magnetic impurities in a paramagnetic host of very low atomic number. In fig.6.2, the anisotropic components, $E_{12}^{11}$-$E_{12}^{\perp\perp}$, have been found to be oscillatory functions of separation $R_{12}$ along both [010] and [110] directions. This suggests that for a random arrangement of magnetic impurities, which is the case of 'ideal' spin glasses, the anisotropic interactions are also random. As already mentioned in the discussion of chapter 6, this new anisotropic frustration effect caused by random anisotropy can be an essential ingredient in the study of ground state properties of spin glasses. Secondly, the size of the anisotropic components contained in the relativistic two site interaction in a realistic host has been determined and found to be remarkably enhanced (for AuFe $\sim 10^{-04}$ Rydberg and for CuFe $\sim 10^{-05}$ Rydberg) compared to the results found by Fert et al (1980) and Staunton et al (1988) (which for two Fe impurities in a jellium model was of the order $10^{-06}$ Rydberg), while the two site interaction itself has been $\sim 10^{-03}$ Rydberg. Thus a realistic treatment of heavy host sites in studying two impurity site interaction has been shown to be crucial and the spin-orbit interaction can no longer be justified as a small perturbation for studying the anisotropic effect in dilute magnetic alloys. Thirdly as in fig. 6.5, for the first time, a weak anisotropic effect with respect to the crystal axes has also been found to be contained in this relativistic two site interaction. So, in this thesis, some completely new features of the interaction between

two magnetic impurity sites and the origin of anisotropic effects have been found.

In section 2.2, the Kohn-Sham-Dirac equation for spin polarised scattering (Strange et al 1984) has been solved incorporating an additional potential term in the relativistic Hamiltonian for a fictional field $\underline{B}^{ext}$ coupling to the current only due to the spin of the electron on the impurity site. The coupling due to the orbital part of the electron is neglected in this approach. For transition metals the spin angular momentum contributes mainly to the effective moment, so the spin polarised scattering theory discussed in section 2.2 is adequate to study the magnetic anisotropy of transition metal alloys. In rare earth metals both spin and orbital angular momenta contribute to the effective magnetic moment and thus the spin polarised scattering theory discussed in this thesis is inadequate to study the magnetic anisotropy of such alloys.

As a technical point the multiple scattering effect vanishes in equation (6.7) for energies with very large imaginary parts ( 1.0 Rydberg) in the Matsubara sum (section 6.3) and the contribution to the interaction energy between two impurities gets negligibly smaller and subsequently the anisotropic component in the two site interaction is destroyed.

Applying the expression (which has been presented in section 6.3) for the relativistic two site interaction, the temperature dependence on the anisotropy field of magnetic alloy can also be studied. As $T \longrightarrow 0^{o}K$, the energy grids calculated from the closely spaced Matsubara frequencies are nearly continuous and the anisotropic effect should be studied by performing a numerical integration of expression (5.24).

The uniaxial anisotropy and the relativistic two site interaction, which has been studied in this thesis, are good starting points from which to study the remanent magnetisation and other spin glass properties of dilute magnetic alloys, like AuFe, because of the incorporation of the full effect of the host sites into the interaction between two magnetic impurities. The inversion symmetry of this relativistic two site interaction would be broken if the interaction had been derived by considering a third impurity site in the realistic host and the resulting anisotropy would then have been unidirectional.

Prejean et al (1980) found that the remanent magnetization $H_r$ for CuMn in spin glass

state is enhanced linearly by the addition of Au or Pt (0.01 to 0.15 at percent) nonmagnetic impurities. This experimental fact can also be studied by deriving a theory for the relativistic interaction between two magnetic impurities (Mn) in a paramagnetic host (Cu) by considering a third nonmagnetic impurity (Au or Pt) following the same procedure used in this thesis to derive the relativistic two impurity sites interaction. The inversion symmetry of this resulted two site interaction about their mid-point will be broken and thus it will provide an antisymmetric unidirectional anisotropic effect. The effect of the concentration of the third nonmagnetic impurities on the remanent magnetization can be investigated by studying the anisotropic effect on the relativistic two site interaction moving a third nonmagnetic impurity (Au or Pt) away gradually. In this case, the anisotropy field may be larger in CuMn(Au or Pt) spin glass alloys because of their dependence on the third nonmagnetic site compared to the anisotropy field in a binary spin glass CuMn.

Ultimately the more complicated theory for the relativistic interaction between many magnetic impurities in a realistic host can also be studied within this framework and consequently, a new insight for dilute magnetic alloys can be evolved and a better understanding on the origin of magnetic anisotropy for such alloy can be achieved.

# Appendix A

From equation (2.47), suppressing the angular momentum quantum numbers,

$$\tau^{ij} = t_i\delta_{ij} + \sum_k t_i G_{ik}\tau^{kj} \tag{A.1}$$

This equation represents the scattering property for a pure metallic system. Now for two pure metallic host sites 1 and 2 this equation gives the following equations

$$\tau^{12} = [1 - t_1 G_{12} t_2 G_{21}]^{-1} t_1 G_{21} t_2 \tag{A.2}$$

$$\tau^{22} = [1 - t_1 G_{12} t_2 G_{21}]^{-1} t_2 \tag{A.3}$$

$$\tau^{21} = [1 - t_2 G_{21} t_1 G_{12}]^{-1} t_2 G_{21} t_1 \tag{A.4}$$

$$\tau^{11} = [1 - t_1 G_{12} t_2 G_{21}] t_1 \tag{A.5}$$

Now, because the host sites are identical, putting $t_1 = t_2 = t_o$ and considering the $t$-matrices for the impurity sites to be $t_1$ and $t_2$ the induced number of states for two impurity sites in a paramagnetic host is

$$N(E) \sim (1 + \tau^{11}(t_1^{-1} - t_o^{-1}))^{-1}\tau^{12}(t_2^{-1} - t_o^{-1})(1 + \tau^{22}(t_2^{-1} - t_o^{-1}))^{-1}\tau^{21}(t_1^{-1} - t_o^{-1}) \tag{A.6}$$

For two impurities embedded in a jellium model $t_o$ can be set equal to zero i.e. $t_o \longrightarrow 0$ and finally

$$N(E) \sim t_1 G_{12} t_2 G_{21} \tag{A.7}$$

Thus the relativistic two site interaction can be reduced to the relativistic RKKY interaction derived by Staunton et al (1988).

## References


Alexander S. and Anderson P. W. 1964, Phys. Rev. 133A. 1594

Anderson P. W. 1959, Phys. Rev. 115. 2

Bansil A. 1975, Solid state Commun. 16, 885

Baym G. 1969, Lectures on Quantum Mechanics W. A. Benjamin. Inc.

Brailsford F. 1966, Physical Principles of Magnetism D. Van Company Ltd. p109

Burdick A. G. 1963, Phys. Rev. 129, no.1, 138

Callaway J. 1974, Quantum Theory of the Solid State B Academic Press, Inc.

Callaway J. and Wang C. S. 1977, Physica, 91B, 337

Cannela V. and Mydosh J. A. 1972, Phys. Rev. B6, 4220

Chikazumi S. 1964, Physics of Magnetism, John Wiley and Sons, Inc.

Christensen N. E. and Seraphin B. O. 1971, Phys. Rev. B10. vol. 4, 3321

Chowdhudi J. and Chatterjee S. 1979, J. Phys. C: Solid state Phys. 12, 2025

Dederichs P. W., Akai H., Blugel S., Stefanou N. and Zeller R. 1987, Lecture Notes, NATO Advanced Study Institute on Alloy Phase Stability, Crete, Greece (June 14-27)

Dzyaloshinsky I. 1958, J. Phys. Chem. Solids 4, 241

Edwards S. F. and Anderson P. W. 1975, J. Phys. F5, 965

Feder R., Rosicky F. and Ackermann B. 1983, Z. Phys. B 52, 31

Fert A. and Levy P. M. 1980, Phys. Rev. lett. 44, 1538

Fetter A. L. and Walecka J. D. 1972, Quantum Theory of Many Particle Systems, New York: McGraw-Hill

Friedel J. 1958, Nuovo Cimento 10, suppll. no. 2, 287

Fritsche L., Noffke J. and Eckardt H. 1987, J. Phys. F: Met. Phys. 17, 943

Frohlich H. and Nabarro F. R. N. 1940, Proc. Roy. Soc. (London) A175, 382

Ginatempo B. Private communication.

Goldberg S. M., Levy P. M. and Fert A. 1986, Phys. Rev. B53, 273

Gunnarson O. 1976, J. Phys. F6, no.4, 587

Gyorffy B. L. and Stocks G. M. 1979, Electrons in Disordered Metals and Metallic Surfaces, ed. P. Phariseau , B. L. Gyorffy and L. Scheire (New York: Plenum)

Gyorffy B. L. and Stott M. J. 1973, Band Structure Spectroscopy of Metals and Alloys, ed. D. J. Fabian and L. M. Watson (Academic Press)

Herring C. 1966, Magnetism, vol.IIB, ed. George T. Rado and Harry Suhl., Academic Press Inc.

Hohenberg P. and Kohn W. 1964, Phys. Rev. 136, B864

Kasuya T. 1956, Progr. Theor. Phys. 16, 45

Kittel C. 1976, Solid State Physics, New York: John Wiley and Sons.

Kohn W. and Rostoker N. 1954, Phys. Rev. 94, 1111

Kohn W. and Sham L. J. 1965, Phys. Rev. 140, A1133

Kohn W. and Vashista P. 1982, Physics of Solids and Liquids, ed. Lundqvist S. and March N. H.

Kondorskii E. I. and Straube E. 1973, Sov. Phys. JETP 36, 188

Korringa J. 1947, Physica 13, 392

Levy P. M. and Fert A. 1981, Phys. Rev. B23, 4667

Lloyd P. and Smith P. V. 1972, Adv. Phys. 21, 89

Loucks T. L. 1967, Augmented Plane Wave Method, W. A. Benjamin, inc.

MacDonald A. H. and Vosko S. H. 1979, J. Phys. C: Solid State Physics 12,2977

Messiah A. 1965, Quantum Mechanics, John Wiley and Sons, Inc.

Monod P., Prejean J. J. and Tissier B. 1979, J. Appl. Phys. 50 (11), 7324

Moriya T. and Yoshida K. 1953, Progr. Theor. Phys. (kyoto) 9, 663

Moriya T. 1960, Phys. Rev. Lett. 4, 5

Moruzzi V. L., Janak J. F. and Williams A. R. 1978, Calculated Electronic properties of Metals (Oxford; Pergamon).

Nagamiya T. and Kubo R. 1955, Advances in Phys. 4, 1

Newton R. G. 1966, Scattering Theory of Waves and Particles, Springer-Verlag, New York, Inc.

Oguchi T., Terakura K. and Hamada N. 1983, J. Phys. F: Met. Phys. 13, 145

Onodera Y. and Okazaki M. 1966a, J. Phys. Soc. Japan 21, 1273

Prejean J. J., Joliclerc M. and Monod P. 1980, J. Phys. (Paris) 41, 427

Rajagopal A. K. 1980, Adv. Chem. Phys. 41, eds. Prigogine I. and Rice S. A. (Wiley), 59

Ramana M. V. and Rajagopal A. K. 1979, J. Phys. C: Solid State Physics 12, L845

Ramchandani M. G. 1970, J. Phys. F 3, 1

Rose M.E. 1961, Relativistic Electron Theory, John Wiley and Sons, Inc.

Ruderman M. A. and Kittel C. 1954, Phys. Rev. 96, 99

Schiff L. I. 1968, Quantum Mechanics, Third edition, McGraw-hill, Inc.

Staunton J. B., Gyorffy B. L. and Weinberger P. J. 1980, J. Phys. F 10, 2665

Staunton J. B., Gyorffy B. L., Poulter J. and Strange P. 1988, J. Phys. C: 21, 1595

Staunton J. B., Gyorffy B. L., Poulter J. and Strange P. 1989, J. Phys.: Condens. Matter 1, 5157

Stefanou N., Oswald A., Zeller R. and Dederichs P. W. 1987, Phys. Rev. B35, no. 13, 6911

Stevens K. W. H. 1953, Revs. Modern Phys. 25, 166

Stoner E. C. 1938, Proc. Roy. Soc. A165. 372

Strange P., Staunton J. B. and Gyorffy B. L. 1984, J. Phys. C: 17, 3355

Strange P., Ebert H., Staunton J. B. and Gyorffy B. L. 1989, J. phys: Condens. Matter 1, 3947

Stocks G. M., Temmerman W. M. and Gyorffy B. L. 1979, Electrons in Disordered Metals and Metallic Surfaces, ed. Phariseau P., Gyorffy B. L. and Schaire L.

Takada S. 1966, Prog. Theor. Phys. 36, 224

Takeda T. 1980, J. Phys. F 10, 1135

Temmerman W. M. 1982, J. Phys. F: Met. Phys. 12, 125

Toulouse G. 1977, Commun. Phys. 2, 115

White R. M. 1970, Quantum Theory of Magnetism, McGraw-Hill, Inc. 44

Walstedt R. W. and Walker L. R. 1981, Phys. Rev. Lett. 47, 1624

Yoshida K. 1957, Phys. Rev. 106, 893

Zener C. 1951, Phys. Rev. 81, 440

TITLE A THEORY FOR DILUTE MAGNETIC ALLOYS — THE ORIGIN OF MAGNETIC ANISOTROPY

AUTHOR MD ABDUS SATTER

INSTITUTION and DATE University of Warwick 1989